Science
AAAS

Supplementary Materials for

Ephemeral stream water contributions to United States drainage networks

Craig B. Brinkerhoff *et al*.

Corresponding author: Craig B. Brinkerhoff, cbrinkerhoff@umass.edu

Science **384**, 1476 (2024)
DOI: 10.1126/science.adg9430

The PDF file includes:

Materials and Methods

All modeling and analysis was performed on the Unity Cluster at the Massachusetts Green High Performance Computing Center (MGHPCC) using publicly available datasets, models, and entirely free and open-source geoprocessing tools in the R programming language. All data and models used in this analysis are described in Table S1.

1 Drainage network framework

1.1 Overview

We use the United States Geological Survey (USGS) National Hydrography Dataset High-Resolution (NHD-HR) built at 1:24,000 map scale (*22*) for our drainage network hydrography. We use the data publicly available as of Spring 2022. This is the highest resolution hydrography data available and is often treated as a gold-standard to benchmark hydrography models against. The NHD-HR is discretized into 'reaches', which correspond to mass-conserved segments of rivers, streams, ditches, canals, lakes, and reservoirs. Note that the NHD-HR often includes estuarine bays within its hydrography. To remain consistent across the United States, we did not separate these waters from the other freshwater rivers. We treat these reaches as part of the CONUS river system, even if they have an estuarine influence. In relevant basins, this will generally provide a more conservative estimate of the ephemeral influence relative to removing these reaches, as it allows for additional dilution by perennial reaches (section 3.1). The NHD-HR uses artificial flowpaths to maintain network topology through lakes and reservoirs, and here we use a previously developed routing framework to handle complex lakes/reservoirs with multiple river inflows during our routing (*23*). The NHD-HR also includes nested drainage basins across 12 levels, where higher level sub-basins are hierarchically nested within lower level basins. As described in the Main Text,

we run our model at each fourth level basin (HUC4), summarizing results at this scale (Fig. 1a). Our mapping validation is done at the 2nd level due to limited in situ data availability in some fourth level basins.

As with all human-built products, NHD-HR data quality varies across CONUS. We identified significantly higher drainage densities in the NHD-HR for the state of Indiana (often 1-2x the stream orders as other portions of a given basin in adjacent states). For these basins, we manually removed the lowest one or two stream orders within the Indiana portions of the basin, until the whole-basin drainage density was visually consistent across state lines. We also remove all divergent reaches, i.e. minor flowpaths that diverge from the main downstream path of flow. We do not remove the rest of the flowpath downstream of a divergent reach if there was another, non-divergent source that joined and made the path no longer divergent. Divergent channels are generally alternative flowpaths in multi-channel rivers, and so we remove them to avoid double-counting rivers.

1.2 Discharge model

Each reach is associated with a mean annual discharge $\bar{Q}$ as modeled by an existing USGS surface hydrology model (*22*). They modeled mean annual runoff by closing a water balance using auxiliary datasets for mean annual precipitation, evapotranspiration (ET), and soil moisture storage. ET losses were not allowed to surpass precipitation. They then overlaid the resulting runoff atop the CONUS catchments and finally routed it downstream to produce mean annual discharge. The routing scheme also accounts for ET losses from the river surface (*22*). While developed for mean annual flow for 1970-2000, we re-validate the model for 1970-2018 to confirm its usefulness over the entire re-analysis period (Fig. S4b). We validate the discharge model for 1970-2018 using all USGS streamgauges with at least 20 years of data within that time period. For additional validation in ephemeral streams, this dataset is supplemented with mean annual flow estimates from USGS streamgauges in ephemeral/intermittent streams, as defined by various workers in USGS reports (*50–54*). For these sites, we do not require at least 20 years of data. To quality control the sites flagged as ephemeral for later use (section 4), we use satellite imagery and hydrograph analysis to manually verify that they are not more representative of an intermittent river, i.e. visual and graphical signs of persistent baseflow, persistently waterlogged soils, riparian zones with rooty vegetation. For all other streamgauges with at least 20 years of data, we identify ephemeral/intermittent streams as those that (on average) run dry at least 5 days a year, acknowledging that sometimes zero-flow readings at streamgauges reflect other scenarios than a dry channel (*55*, *56*). Validation results are discussed in Supplementary Materials S1 and plotted in Fig. S4b. In total, we validate the discharge model at 4,053 rivers.

It is worth noting that ephemeral streams establish losing conditions when flowing, i.e. the direction of the hydraulic head facilitates 'transmission losses' of water from river channel to soils and eventually groundwater (*57–59*). Transmission losses from ephemeral streams are generally of two types: groundwater recharge or evapotranspiration from the water surface and riparian corridor. In arid basins, the latter generally dominate transmission losses (*59*). The discharge model and flow accumulation procedure that we use (*22*) accounts for evapotranspirative transmission losses on an annual timescale, using a model of excess evapotranspiration from the river corridor for arid basins. For non-arid basins, infiltration of ephemeral flow often recharges catchment groundwater and resurfaces several stream orders downstream (*60*). The discharge

model does not explicitly account for this phenomenon in its flow accumulation procedure. Despite this, the model's estimation biases were approximately similar across perennial and non-perennial rivers (Fig. S4b). This is presumably due to other model uncertainties outweighing the uncertainties associated with transmission losses. Because these biases are similarly distributed, and we use relative metrics such as the percent of total flow when reporting results, uncertainties associated with ephemeral transmission losses likely do not meaningfully influence our conclusions at this scale.

1.3 Hydraulic Geometry

We use hydraulic scaling to obtain estimates of bankfull river depth and mean annual lake/reservoir depth (necessary to assess ephemerality- Section 3.1). For rivers, we use the relation from (*21*), who fit equations of the form $H_b = aA_c^b$, where H_b is field-measured bankfull depth and A_c is the river's drainage area, to eight physiographic regions across the United States (Fig. S30). They had over 1,300 sites in total with field-verified bankfull depths to fit their regional models. For lakes and reservoirs, we use mass-conservation to obtain average depths from lake/reservoir volume (*Vol*) and surface area *SA*. *Vol* was scaled using an equation of the form $Vol = a(SA)^{1.2}$ (*61*), developed using a global dataset of lake morphometry and the Hurst coefficient for self-affine surfaces.

1.4 In situ data on stream ephemerality

We use a dataset of in situ assessments of 'stream ephemerality' to validate our stream classification model. This dataset comes from three sources: 1) EPA WOTUS jurisdictional determinations, 2) USGS streamgauges, and 3) field assessments of New England streams. Each dataset is described below.

The EPA 'Waters of the United States' (WOTUS) jurisdictional determinations dataset (*62*) consists of field assessments performed by EPA workers made at landowners' requests, where status was determined under the at-the-time definition for WOTUS extent. We use the data available as of 06/20/2022 when downloaded. We filter this dataset to include only determinations made under the Navigable Waters Protection Rule (NWPR- *30*) after it was enacted in 2020, which includes an explicit category for ephemeral streams. This amounts to over 60,000 distinct jurisdictional determinations (often including multiple determinations in the same reach, over space and time) and forms the bulk of our dataset. To make the dataset copacetic with our model, we remove data not associated with surface water features directly connected to the drainage network: adjacent/riparian wetlands, drylands, upland terrestrial sites, upland or non-adjacent wetlands/ponds/depressions, croplands, wastewater plants, and groundwater. We retained all other determinations that are directly connected to the drainage network (rivers, lakes, reservoirs, canals, ditches, stormwater control features, and artificial surface water features) and recast all determinations as ephemeral or non-ephemeral.

We supplement the jurisdictional determinations dataset with the USGS streamgauge network. Because the EPA jurisdictional determinations are done on a voluntary basis at landowners' requests, it is biased towards waterbodies whose WOTUS status is not so easily discerned. Thus, the EPA jurisdictional determinations rarely include larger (usually perennial) rivers. To make sure we are also correctly classifying larger rivers, we include gauged rivers (section 1.2) in our

validation. All gauged rivers that, on average, are flowing 95% of the year are conservatively assumed to be non-ephemeral, and are added to the dataset as such.

Finally, we manually assess stream ephemerality in northeastern CONUS because our validation data includes no ephemeral reaches in this region. We follow the 'expert protocol' used by North Carolina's department of Water Quality for assessing stream ephemerality (*63*). This protocol uses geomorphic, hydrologic, and biotic indicators of seasonally and/or permanently high water tables to assess stream permanence. We use our local knowledge to identify streams we thought are likely to be ephemeral, verify they are present in the NHD-HR (but did not look at the model result a priori to avoid biasing our assessments) and assess the channels following the protocol. Classification results are in Table S4 for the five sites. All streams are assessed over 48 hours from the most recent rain event to avoid the influence of delayed runoff in the channel that might be mistaken for baseflow. Note that we do not perform full soil assessments nor species counts as the protocol technically specifies, but instead perform rapid visual assessments that favor speed of classification over thoroughness. Per the protocol, none of these channels are close enough to being classified as intermittent (Table S4) that we feel confident our rapid assessments are sufficient. While we only assess five ephemeral rivers, they provide at least some validation data in northeastern CONUS.

We join the three datasets to the NHD-HR by snapping each field assessment to the nearest reach. Despite its high resolution, the NHD-HR does not contain every stream in CONUS and many of the field sites are not expected to be associated with a reach. We settle on a threshold of 10m. The tests and rationale used to drive this decision are explained in section 3.3. After snapping, we assign the most frequently occurring field assessment along the reach as its 'true assessment of ephemerality'. If there is a tie between frequency of occurrence (meaning there is no consensus on whether the reach is ephemeral or non-ephemeral), we remove those points from the dataset. Ultimately, we have 7,207 field assessments of reach ephemerality to validate our model. Fig. S5b maps the regional distribution of these data.

2 Calculating ephemeral contributions

We calculate the ephemeral percent of discharge (equation S1) and drainage area (equation S2) for all 20,708,899 reaches by routing through the drainage network from upstream to downstream. When a basin discharges into a downstream drainage network, we pass the exporting reach's value to the downstream basin's corresponding reach. Routing between basins was facilitated by a custom routine which runs the drainage network routing in parallel across basins at the same 'processing level' and then passes exported parameters of interest to the basins immediately downstream in the next processing level. To calculate the basin-exported values for equations S1 and S2, we sum up the ephemeral percentages at all terminal reaches in the basin (sometimes rivers terminate endorheically and occasionally basins have two or more outlets) and then re-calculate equations S1 and S2. We also calculate the mean annual ephemeral flow frequency (equation S3, section 4).

More specifically, the ephemeral contribution to discharge E_Q (equation S1) is the average of each discharge source's ephemeral contribution, weighted by discharge to favor larger water sources. k refers to each reach directly upstream and Q_l is the lateral runoff contribution from the current reach's catchment. E_{Q_l} is set to 1 for ephemeral streams and 0 for non-ephemeral streams. For

losing streams (when discharge decreases downstream due to evapotranspirative losses or groundwater seepage), E_{Q_l} is set to 0 as there is no lateral contribution into the stream channel. Equation S1 is mapped in Fig. 1a.

$$E_Q = \frac{\sum_{k=1}^{K}(E_{Q_k}Q_k) + E_{Q_l}Q_l}{\sum_{k=1}^{K}(Q_k) + Q_l} \textbf{(S1)}$$

The ephemeral percent of drainage area E_A (equation S2) is the average of each discharge source's ephemeral drainage area, weighted by drainage area to favor larger water sources. *A* is the upstream drainage area. Equation S2 is mapped in Fig. S29.

$$E_A = \frac{\sum_{k=1}^{K}(E_{A_k}A_k) + E_{A_l}A_l}{\sum_{k=1}^{K}(A_k) + A_l} \textbf{(S2)}$$

Finally, we calculate basin-average ephemeral flow frequency N_{flw} (equation S3) as the percent of an average year (in days) that ephemeral streams are flowing, where *i* is mean daily runoff depth and i_{min} is an operational runoff threshold for day *d* in the 27-year record *Y*. This calculation is elaborated on in section 4. Equation S3 is mapped in Fig. 3a.

$$N_{flw} = \sum_{y=1}^{Y=27}\left(\sum_{d=1}^{D=365}(i \geq i_{min})\right)/27 \textbf{(S3)}$$

3 Identifying ephemeral streams

3.1 Model

We use a ~1km global soil hydrology model for mean monthly estimates of the water table depth (*WTD*)(*19*, *20*). This model solves a vertical soil water balance as inferred from remotely sensed leaf area index (*20*). It ignores local, perched aquifers and anthropogenic pumping in favor of a broad, long-term average *WTD*, as is common in global-scale groundwater models (*64*, *65*). Ignoring pumping likely leads to an underestimation of ephemeral streams, as the modeled water table is artificially high relative to the observed water table that has been lowered by pumping. Under these cases, we likely mis-classify ephemeral streams as perennial and thus underestimate the total ephemeral influence in an intensively pumped region. To quantify the influence of using a coarse, global-scale groundwater model, we validate it against in situ mean monthly water table depths (62,000+ observations over 12 months at 5,228 sites). We use only USGS groundwater wells and USGS stream gauges with at least twenty years of data. We use stream gauges that flow 100% of the time to validate places where the water table should be approximately 0m deep (while an approximation, this provides a much more representative validation dataset). The results of this validation are described in Supplementary Materials S1 and Fig. S8.

Definitions for ephemeral and non-perennial streams vary considerably across scientific communities, regulatory communities, and jurisdictions. For example, the U.S. EPA allows states to adopt different definitions for ephemeral and intermittent streams (*66*) and these definitions are frequently changing (*67*). For the purposes of this study, we use the US EPA's standard working definition for ephemeral streams: ephemeral channels only flow in direct response to precipitation

(e.g. *30*). More intuitively, ephemeral streams 'fill up' while intermittent streams 'run dry'. We confirm this definition is also used across all of our validation data for consistency.

Because ephemeral streams flow only in direct response to rainfall, it follows that there is no sustained stream-groundwater connection to facilitate baseflow in ephemeral channels. Thus, we assume that ephemeral stream channels must be perched above the water table over the entire year (Fig. S1). This theory underpins our entire ephemeral classification model. To apply this theory, we extract the median *WTD* along all 20,708,899 discrete reaches for all 12 months. We then compare each monthly water table depth to the bankfull depth: the 'depth to channel bottom'. If the water table is deeper than the 'depth to channel bottom' for all 12 months, the river is classified as ephemeral (see Fig. S1 for an overview flowchart of the model). To avoid mis-classifying streams with an intermittently high/low water table, this must hold true for all twelve months of the year. We treat all 'main ponded waters', i.e. lakes/reservoirs $\geq 0.01 km^2$ (*68*), as non-ephemeral to ensure that perennial waterbodies are not mis-classified.

Then, we route through the network from upstream to downstream and amend our initial classification to a more conservative estimate. Specifically, if a drainage path has a perennial/intermittent river or main ponded water immediately upstream of it, the current reach must also be non-ephemeral. It is well established that losing streams can lead to disconnected flowpaths at given points in time when their subsurface is able to accommodate all of the flow (*69*). When integrated over annual timescales, any amount of intermittent surface-groundwater connectivity will contribute groundwater-sourced flow to the immediately downstream channel, rendering it non-ephemeral (at least for how we have defined ephemeral streams over annual timescales). Endorheic outlets are already accounted for in our model. We also handle two other scenarios:

- We only count rivers/streams as ephemeral and recast all canals, ditches, and small ponds (waterbodies $< 0.01 km^2$) as non-ephemeral. These features fall under different WOTUS rules and are not the focus of this study.
- While Mexican and Canadian ephemeral streams contribute discharge to the CONUS drainage network, our focus is on CONUS rivers. These streams are thus recast as non-ephemeral. If these foreign streams are larger than first order, however, we assume they are non-ephemeral and thus the model sets the CONUS stream they flow into as non-ephemeral.

3.2 Validation

Ephemeral classification accuracy is assessed using the in situ ephemerality dataset (Section 1.4). We assess performance using regional classification accuracy, sensitivity (the true positive rate), specificity (the true negative rate), and "informedness", which is also called the true skill statistic (*TSS*) or Youden's *J* depending on the literature (*70*). See Table S3 for metric definitions. *TSS* is equal to the sensitivity + specificity - 1. It intuitively represents the performance improvement over a random classifier, i.e. a score of zero indicates that the model is equivalent to random guessing. Mathematically, *TSS* equals the distance (in units of sensitivity) between a point on the receiver operating characteristic (ROC) curve and a random classifier. *TSS* is more robust to class imbalances than simple percent accuracy and it has been used in the past to assess headwater and ephemeral mapping models (*11–13*). We therefore use it here as well to compare against existing

studies. Regional accuracy is mapped in Fig. S4, regional *TSS* is mapped in Fig. S5, regional sensitivity and specificity are mapped in Fig. S3, and boxplots of all metrics are Fig. S7. The validation results are discussed in Supplementary Materials S1.

3.3 Choosing a validation snapping threshold

In general, classification performance should decrease as the snapping threshold increases because the in situ data will be assigned to the wrong rivers. So, we test the sensitivity of our model to this threshold to inform our choice of parameter value.

First, we re-project all data using the Universal Transverse Mercator (UTM) projection system to ensure snapping distances are regionally accurate. Then, we test a range of snapping thresholds from 5m to 50m and assess ephemeral classification accuracy (Fig. S10). We also test which snapping thresholds reproduce expected network scaling patterns according to Horton's law of stream numbers (*71*). Equation S4 is the Horton law of stream numbers, which is a power-law function relating stream order SO_m to the number of streams in the m^{th} order N_m (*71*). R_B is the Horton ratio and N_{max} is the number of streams in the largest order. R_B is solved via least-squares regression.

$$N_m = N_{max} * R_B^{SO_{max} - SO_m} (\mathbf{S4})$$

We fit equation S4 to our in situ ephemerality data after snapping to the NHD-HR using some threshold. We then assess how well the observed N_m (section 1.4) matches the N_m predicted by Horton's laws (equation S4). This approach assumes the following:

- Ephemeral streams aggregated from many CONUS drainage networks will fit a single Horton scaling. Horton laws are a statistical inevitability of stream ordering and do not represent an inherent geomorphic process (*72–74*), but rather arise from hydrography resolution and channelization definitions. Because we use a CONUS-scale product with consistent stream ordering, this is reasonable.

- The in situ ephemerality data (section 1.4) is representative of the actual distribution of ephemeral streams across CONUS. Because these data consist of voluntary field assessments, it is likely an underestimate of ephemeral stream presence. Actual estimates are presumably even greater.

Overall, we find that the ephemeral river network most closely matches expected network scaling with a snapping threshold of 5-15m (Fig. S11). Otherwise, this scaling relationship begins to break down. Taking Figs. S10-S11 in aggregate, we find a snapping threshold of 10m to be most appropriate for our purposes. This threshold also conveniently allows a direct comparison against the only existing ephemeral classification model (*12*), built using 10m gridded flow accumulation data.

3.4 Influence of hydrography resolution

Given that much of the in situ ephemerality data does not fall on the mapped drainage network and instead corresponds to streams too small to be explicitly represented in the NHD-HR, we also assess 1) the amount of ephemeral streams we are missing, and 2) whether this matters for our goals of quantifying ephemeral contributions to CONUS discharge. To do this, equation S4 can be

re-expressed as equation S5 to calculate the ephemeral stream orders not represented in the NHD-HR, where *k* is the minimum stream order. The in situ ephemerality data (section 1.4) provides us with N_k enabling the direct calculation of SO_k. This approach assumes that all streams in the scaled stream order(s) are ephemeral. Given that 84% of CONUS 'source reach' extent is ephemeral in our model, it is reasonable to assume that everything upstream of these is also ephemeral.

$$SO_k = \frac{log(N_k) - log(N_{max}) - SO_{max} log(R_B)}{-log(R_B)} \quad (\mathbf{S5})$$

Using equation S5, we find that one additional ephemeral stream order would need to be added to the NHD-HR to reproduce the field data distribution (Fig. S12). The likely significant omission errors in the in situ ephemerality data suggest that one additional stream order is a conservative estimate. This has different implications for our various results. Because discharge generally accumulates downstream, we can assume that our model's headwater ephemeral discharge contributions (Fig. 2a) implicitly include the scaled ephemeral stream order as well, despite not being explicitly mapped in the NHD-HR. This may inflate the influence of first-order streams (Fig. 2a), but it does not influence the basin-wide results (Fig. 1). However, it does significantly affect our ephemeral network extent (Fig. 4), which should be taken as a conservative estimate as we cannot verify how many ephemeral orders might lie above the NHD's 'first' order streams.

4 Estimating ephemeral flow frequency

We estimate the basin-average flow frequency of ephemeral streams via the mean annual number of days per year that they flow (N_{flw}- equation S3). We do this using mean annual, basin-averaged runoff data measured at streamgauges (*43*) and 27 years of daily interpolated precipitation data for 1980-2006 (*42*, *75*). The model is purposefully simple but globally scalable (Fig. 3).

4.1 Data

We use field data only to determine an operational runoff threshold, as well to verify the model's performance. Note that in situ N_{flw} data is relatively uncommon and measured using different sensors (streamgauges, temporary flumes, and electrical resistance senors). To our knowledge, we use all existing field data (*76–83*) that provides sufficient information to calculate N_{flw} (Table S2 details the studies). We also supplement this data with the ephemeral USGS streamgauges previously described in section 1.2. To get all data in a uniform format, we calculate mean annual N_{flw} at each sensor (if applicable), and then take the catchment average N_{flw} across the sensed streams (again, if applicable). This averaging was not done in catchments with insufficient data and therefore significant uncertainties exist in many of these estimates. Despite these uncertainties, this limited data is to our knowledge the largest collection of in situ N_{flw} measurements.

Length of the timeseries varies significantly, from approximately 1/3 of a year (*83*) to 45 years of sub-daily data in the Walnut Gulch Experimental Watershed (*80*). Data from (*83*) exist for three sites within a catchment in Ontario that do not flow into the United States. However, they are located approximately 15 km from one of our model basins that does flow into the United States (Fig. 3a) and so we use that basin for verification. Additionally, that data is only for 1/3 of the year (approximately July to October). To obtain a mean annual estimate, we assumed the frequency of flow was the same year round, i.e. we tripled the N_{flw} measured in their study. Likewise, (*77*) only assessed their streams for the latter half of a year, though reports indicate that flow generally occurs

only 1-2 times in the remaining months (*84*), so we added that to the calculation. Finally, one site (*76*) includes an intermittent main stem where the flow was measured, however the rest of the drainage system is ephemeral (*76*).

4.2 Model

Streams are traditionally viewed as a surficial expression of groundwater (*57*). However, by definition ephemeral streams extend beyond the boundary of the surface extent of groundwater (*85*). Because they have no groundwater component, N_{flw} is purely controlled by surface runoff and interflow. This assumption significantly simplifies our modeling and enables the estimation of N_{flw} solely via surface runoff generation.

In that context, we first calculate a mean annual basin runoff ratio i_r to convert precipitation *P* to stream runoff *i* and vice versa. The runoff ratio (equation S6) reflects the proportion of rainfall on the basin that winds up as stream runoff, where the implicit losses are via groundwater recharge and evapotranspiration. Using a mean annual i_r also implicitly accounts for snowmelt runoff in winter.

$$i_r = \frac{i}{P} \textbf{(S6)}$$

We convert daily precipitation depth to daily, basin-averaged stream runoff depth using i_r. Per equation S3, streamflow occurs when daily runoff exceeds some operational runoff threshold. We tally all days when flow occurs over the 27 years and calculate a mean annual N_{flw}, which is mapped in Fig. 3a. For a handful of basins on the Mexican/Canadian borders, there are no USGS gauges and no i_r data. We use the mean annual runoff values from adjacent basins (the "closest" as assessed visually) and assume it holds constant in these basins. We perform a sensitivity test of the i_r data, as it is biased towards gauged, often larger, rivers. For this test, we use equation S3 and run the model under four scenarios: inflating and deflating the runoff ratio by 18% and 33%. Across CONUS, results change minimally (Fig. S13).

We also parameterize watershed 'memory': a bulk parameter representing all delayed runoff to the drainage network. More practically, the memory parameter keeps streams 'turned on' for a number of days following a day identified as flowing. Memory parameter assignment was guided by a recent analysis (*86*), which calculated the streamflow memory of rain events for 671 watersheds in CONUS (including many with groundwater influence). They found a median memory of approximately four days, which is used here.

The operational i_{min} is determined using the N_{flw} field data (section 4.1) as (to our knowledge) there is no consensus on what runoff depth defines a flowing stream and even then there are known limitations to measuring low flows in the field (*56*). Further, the coarse spatial resolution of our precipitation data can't reconcile sub-pixel heterogeneity and thus limits our ability to remotely sense the smallest runoff events (potentially inflating the smallest rain events at the sub-pixel scale). So, we calibrate i_{min} in lieu of other available data, acknowledging that this operational definition of i_{min} may change with additional field measurements of N_{flw}. We use the coefficient of determination r^2, the mean absolute error (*MAE*) and the root mean square error (*RMSE*) to determine the best performing i_{min} of approximately 2.5 mm/day (Fig. 3b-c, Fig. S31). We express uncertainty in the average estimate as 1 standard error (SE) of the regression between predicted

and observed. We stress that because of the limited and highly uncertain data on N_{flw} and the necessary calibration of i_{min}, we refer to this as a model verification: all we can do is confirm that the model is reasonably realistic.

Supplementary Materials S1

Discharge model performance

The discharge model accurately captures mean annual discharges for 1970-2018 across both perennial and non-perennial streams (Fig. S4). This performance is similar to another discharge model used to map global river intermittency (*8*).

Groundwater model performance

The log-residuals of the groundwater model validation (Fig. S8) show reasonable performance for a global model. The resulting errors are similar to the previous global validation of this model (*19*, *20*) and other similar models (*64*, *65*). The small bias underestimating the water table depth (mean residual of -0.236 meters) is likely due to not simulating groundwater pumping. This leads to an underestimation of ephemeral streams which is discussed in the Main Text.

Ephemeral classification performance

Ephemeral mapping performance varies across the United States. Regional average *TSS* is 0.66 (Fig. S5a), average regional accuracy is 86% (Fig. S4a), average regional sensitivity is 81% (Fig. S6a) and average regional specificity was 86% (Fig. S6b). Performance is best in northeastern CONUS and western CONUS (average *TSS* of 0.79), while performance is worse in the Ohio and Lower Mississippi river basins (average *TSS* of 0.42). Overall, we outperform the only two existing CONUS ephemeral stream maps. (*12*) reported a CONUS *TSS* of 0.45, sensitivity of 63%, and specificity of 83% and (*14*), who mapped ephemeral streams using deep learning models for thousands of locations around CONUS, reported an ephemeral classification accuracy of 75%.

Overall performance in an ephemeral catchment

The Walnut Gulch experimental watershed in Arizona is home to one of the longest continuous ephemeral streamgauge records in the world and features an in situ flume network that enables whole-watershed studies for arid hydrology (*80*). The entire watershed drainage network is ephemeral. Here, we verify that our model 1) reproduces the completely-ephemeral drainage system (Fig. S9a) and 2) reproduces the mean annual ephemeral discharges throughout the drainage network (Fig. S9b).

Equations S1 and S2 performance

At continental scales, it is impossible to validate equations S1 and S2 in a traditional sense. To broadly verify that our calculations make sense, we use Tokunaga ratios to compare our modeled metric to an independent, back-of-the-envelope metric obtained from Tokunaga scaling (Fig. S4c). This approach we extends previous work (*17*) that used Tokunaga network scaling in the northeastern US to verify relative headwater contributions to downstream discharge. Tokunaga ratios represent the average number of upstream reaches that flow into the average reach per stream order (*17*, *34*). Assuming that discharge accumulates downstream, relative ephemeral Tokunaga

ratios should be approximately similar to our routing calculations, i.e. if 50% of upstream rivers are ephemeral, than 50% of discharge would be ephemerally sourced in a perfectly gaining watershed.

To do this, we calculate the average cumulative length of upstream ephemeral rivers per stream order. We use network length rather than number of reaches to handle the artificial paths necessary to incorporate lakes and reservoirs into the drainage network (*23*). For the largest stream order, we then divide this value by the total network length to obtain a relative upstream contribution to the watershed mouth. When compared against our moddel (Fig. S4c), we confirm our results are in line with those obtained independnetly by network scaling theory. This provides additional confirmation that our model produces reasonable metrics.

Potential uncertainties

Potential model uncertainties center on the bankfull depth model and the water table model.

For the water table model (*19*, *20*), uncertainties come from (1) general model performance and (2) the model's spatial resolution (~1km). For the former, we validate the mean monthly water table depths at over 5,000 sites (over 60,000 total validation points for 12 months) across CONUS and define a log-error distribution (mean: -0.236m, sd: 0.678m), see Fig. S8. For the latter, our two primary concerns are resolution misalignment between the hydrography and the groundwater model and/or spatial misalignment, i.e. errors in river location in steep terrain might map streams into the 'next pixel over'.

For resolution misalignment, we use the Cedar Brook Catchment in New Hampshire's White Mountains (Fig. S15) as an illustrative example to show the groundwater model resolution (~1km) compared to the NHD-HR hydrography resolution (average reach length across all CONUS basins of 1.8 km). The approximately equal resolutions suggest that it is not a significant source of error. Also note that resolution uncertainty is already implicit in our groundwater validation: we validated point-based well depths against a ~1km gridded model (Fig. S8). This will capture any resolution-induced errors between wells and the model.

Spatial misalignment is reasonably handled by our summarizing along the reaches: when there are multiple pixels along a reach, we take the median water table value to capture a representative, reach-scale picture of water table depths (Fig. S15) that are robust to misalignment. Finally, recall that after the initial classification comparing 'depth to channel bottom' to 'depth to water table', we use network routing to fix any artifacts that might arise from errors in the water table model. These steps in the algorithm significantly reduce the influence of potential resolution errors.

For the bankfull depth model, uncertainties come from (1) statistical performance of the power-law scaling and (2) the specific field measurement dataset used to fit the scaling relationship. (1) is an error of how well a power law represents bankfull depth, which is influenced by the fact that studies establishing this power law come from well-behaved alluvial systems that aren't necessarily representative of all streams (particularly steep headwaters). (2) provides the degrees of freedom, scale, and heterogeneity to assess (1). To quantify this, we use the log-residuals of (1) to characterize error distributions per physiographic region (mean range: 0-0m, sd range: 0.12-0.254m) using the most extensive dataset to our knowledge of in situ bankfull depth measurements (*21*). This dataset includes field-measured bankfull depth in a range of rivers, from large (100+m wide) well-behaved channels to smaller ones less than a meter wide. While there are still

uncertainties baked into this approach, we feel it is the most robust we can produce given the currently available data.

Quantification of uncertainty

We use Monte Carlo simulations to quantify the uncertainty in our main results (Figs. 1, Eq S1). Specifically, we push the two uncertainties defined above for water table depth (Fig. S8) and bankfull depth (*21*) through the entire modeling pipeline to build distributions of model results (Fig. S8). It is computationally infeasible to do this for the entire CONUS domain, so we focus on five smaller drainage basins that cover the major physiographic regions of the United States. For each reach, we randomly sample both error terms, add them to the modeled values, and run the pipeline. We did this 1,000 times in each basin.

In these five test basins, we find that our model results vary very little and that the standard deviation of these uncertainty distributions is < 1% (Fig. S14). This suggests that uncertainties in the bankfull depth and the water table depth only marginally affect the final results. In the Suwannee basin in Florida/Georgia, where much of the water table is very shallow, uncertainties are slightly greater but still well within acceptable values (Fig. S14).

Supplementary Figures

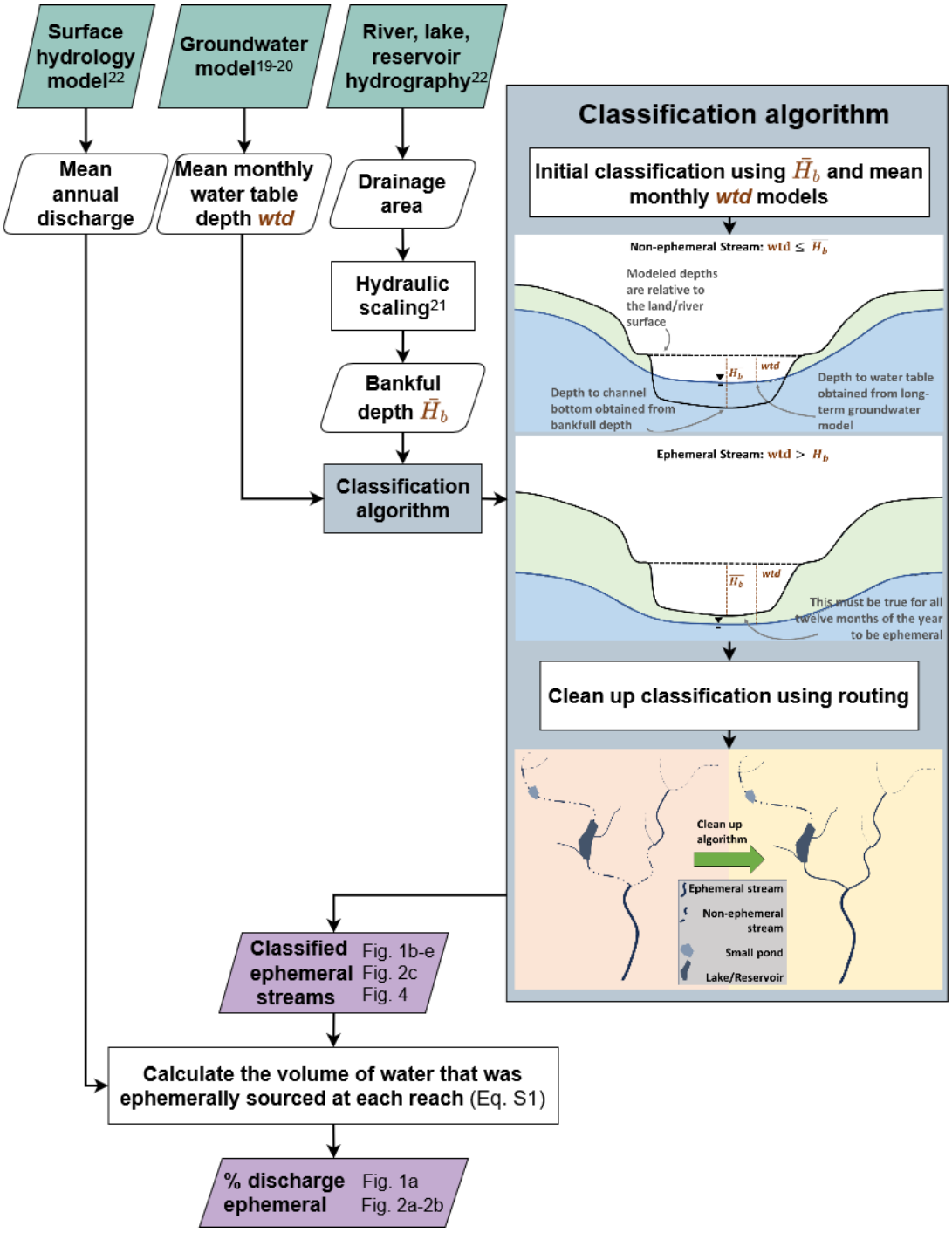

Figure S1: *Flowchart of ephemeral classification algorithm. Green are data inputs to our model. Purple are model outputs. Grey box is the actual classification algorithm. Superscripts refer to references for off-the-shelf data/models. When appropriate, we point to the figures for each result. See Methods for more detail.*

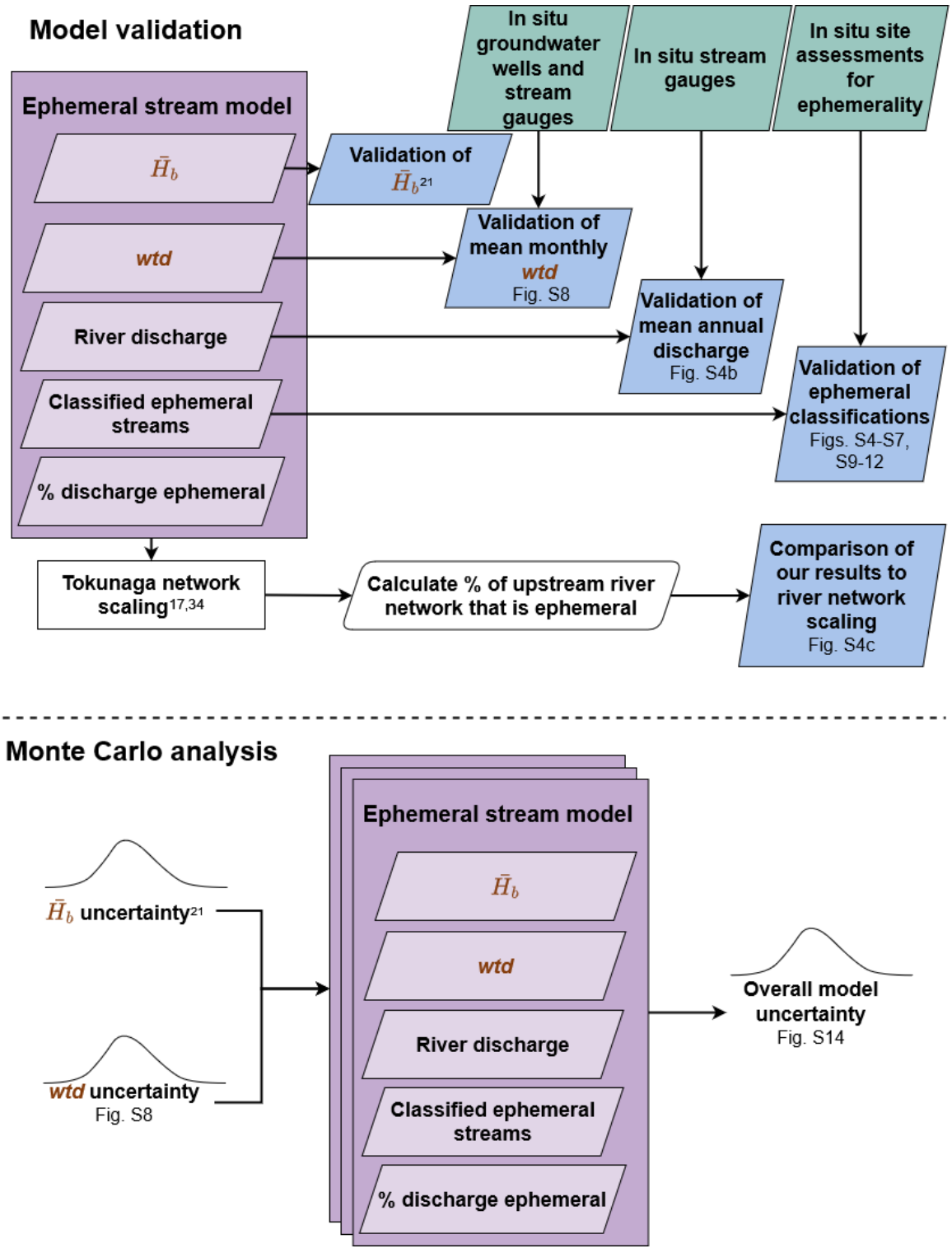

Figure S2: *Flowchart of study validation and uncertainty analysis. Green are independent data used for validation. Purple indicates model outputs. Blue are validation outputs. Superscripts refer to references for off-the-shelf data/models. When appropriate, we point to the figures for each result.*

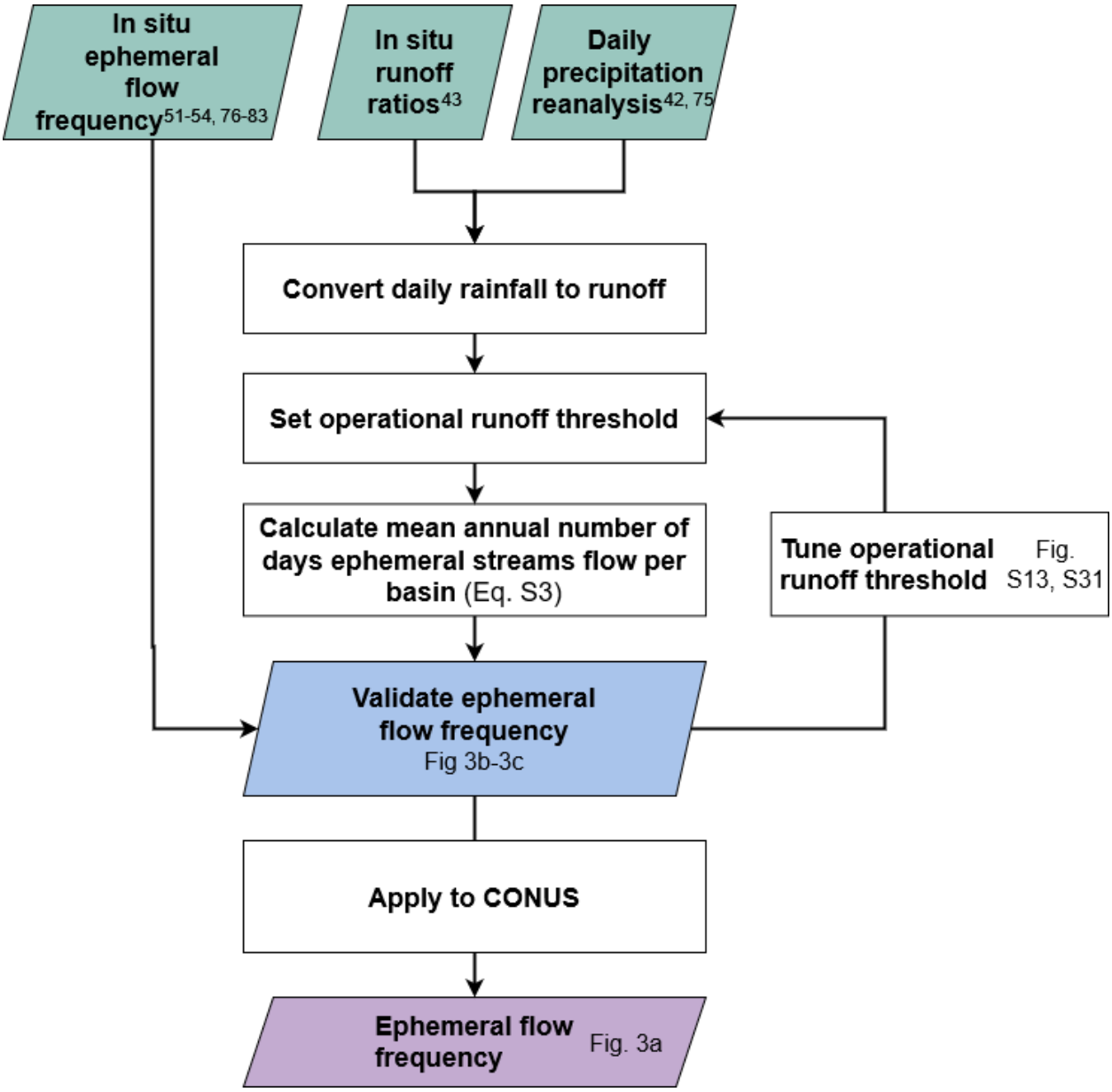

Figure S3: *Flowchart of ephemeral flow frequency analysis. Green are data inputs to our model. Purple are model outputs. Blue are validation outputs. Superscripts refer to references for off-the-shelf data/models. When appropriate, we point to the figures for each result. See Methods for details.*

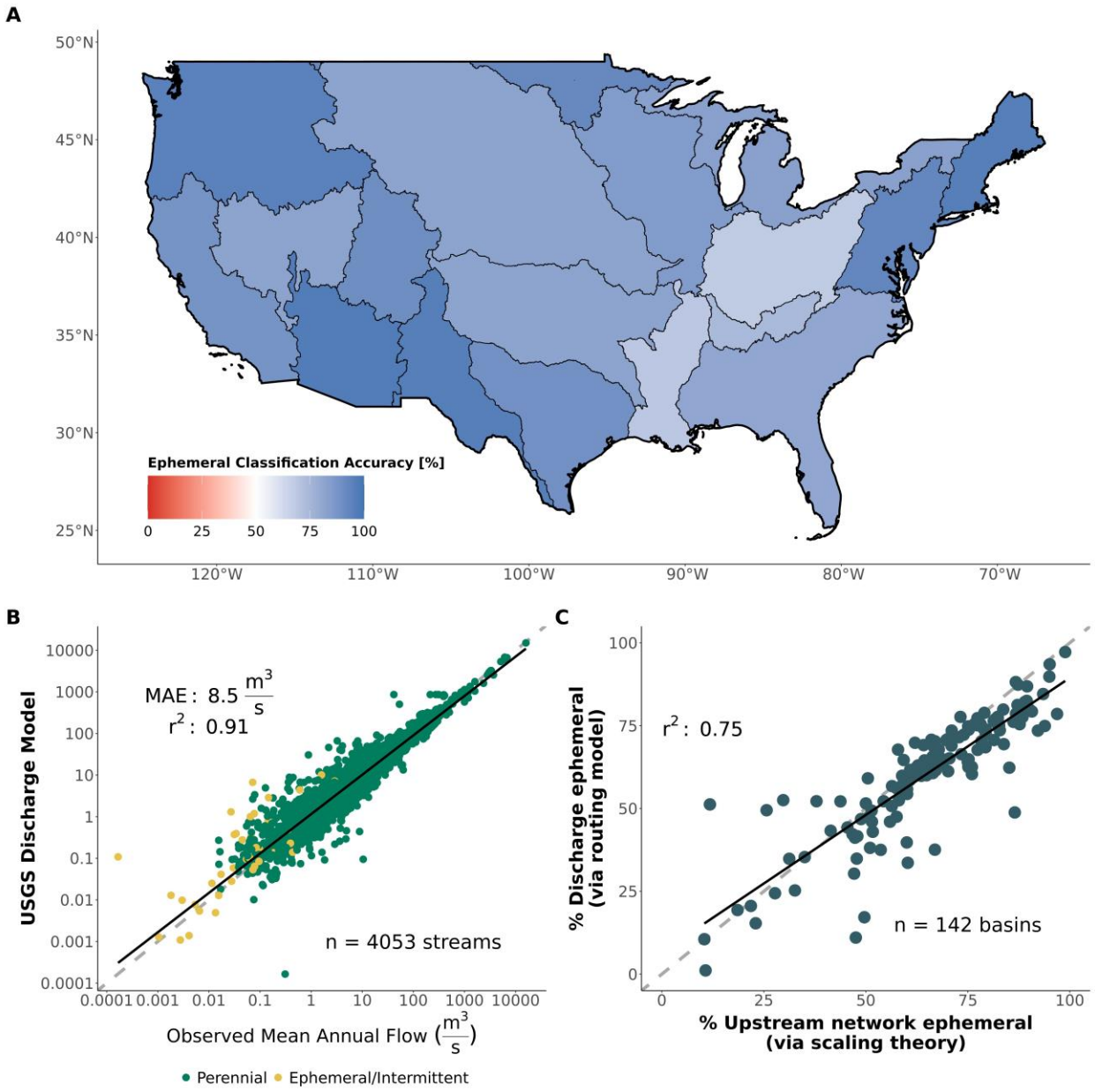

Figure S4: *Main validation of the primary model components: (A) Regional classification accuracy of the ephemeral stream map against approximately 7,000 independent in situ assessments of stream ephemerality. (B) Validation of mean annual discharge model at approximately 4,000 streams across CONUS. Note that some of the non-perennial sites were manually snapped to the NHD-HR to provide additional discharge validation. For quality control, these sites correspond to those with reported drainage areas within 20% of the drainage areas reported in the NHD-HR. (C) Verification that equation S1 is theoretically anticipated by network scaling theory. Only basins completely within the United States are used for this verification- see Supplementary Materials S1 for details on the calculation. Dashed grey lines are the 1:1 lines while black lines denote the linear regression.*

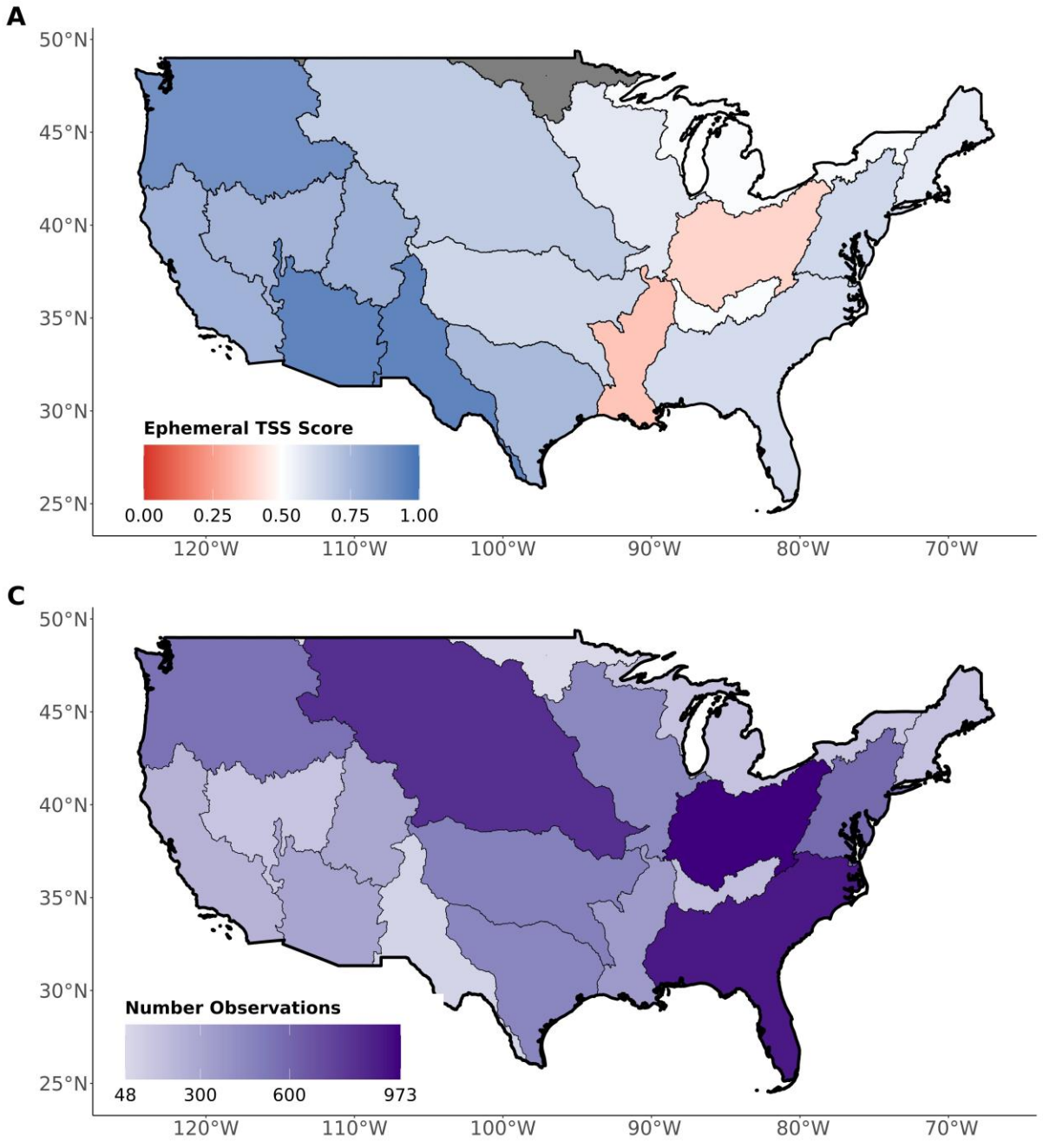

Figure S5: *Regional validation of the ephemeral stream map against approximately 7,000 independent field assessments of stream ephemerality: (A) regional model true skill score (TSS) and (B) number of field-observations per region. See Table S3 for metric definitions. The greyed-out region ('Souris-Red-Rainy basin') has no ephemeral validation data. See Supplementary Materials S1 for more details.*

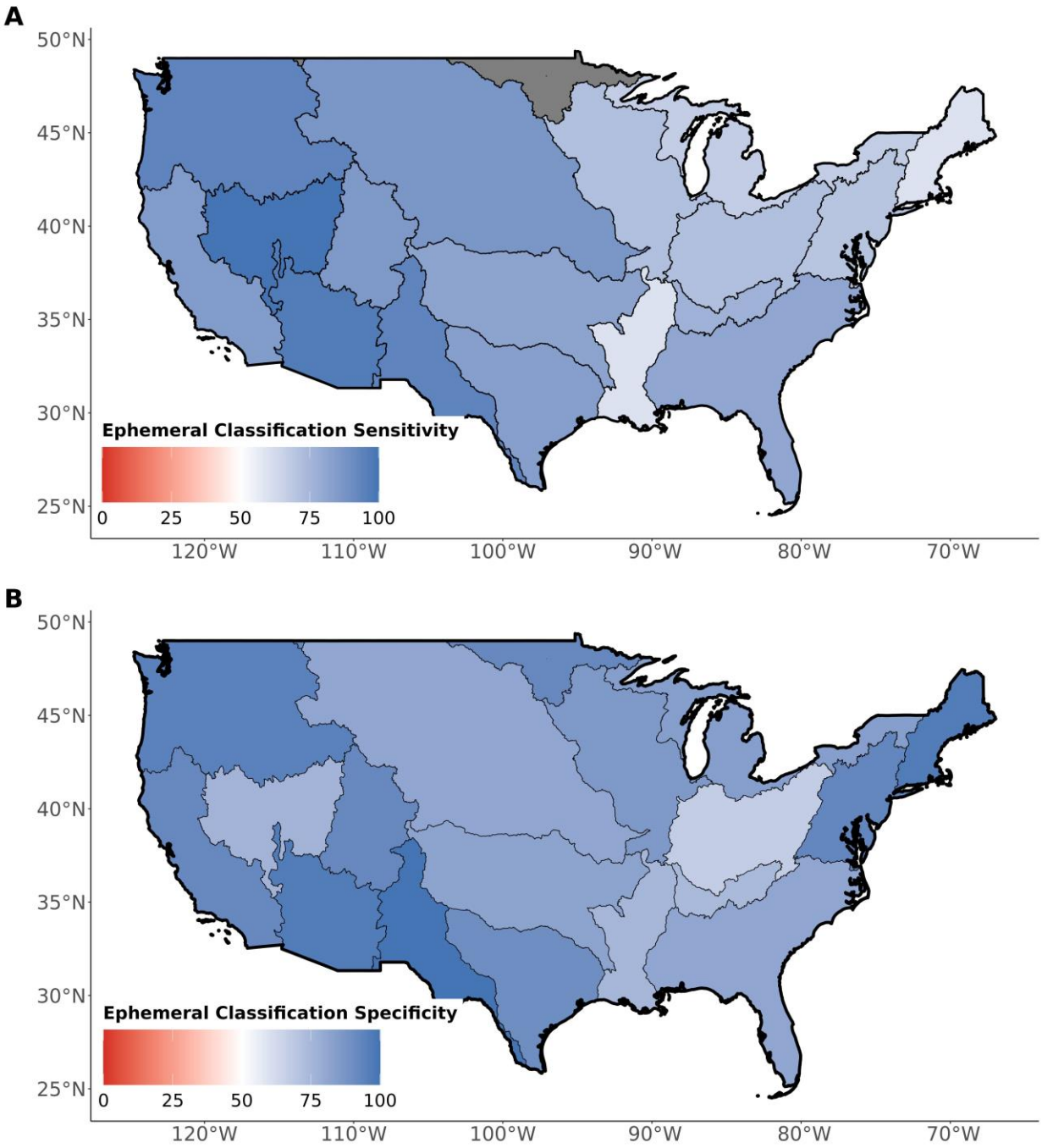

Figure S6: *Regional validation of the ephemeral stream map against approximately 7,000 independent field assessments of stream ephemerality: (A) regional model classification sensitivity and (B) specificity. The greyed-out region ('Souris-Red-Rainy basin') has no ephemeral validation data. See Supplementary Materials S1 for more details.*

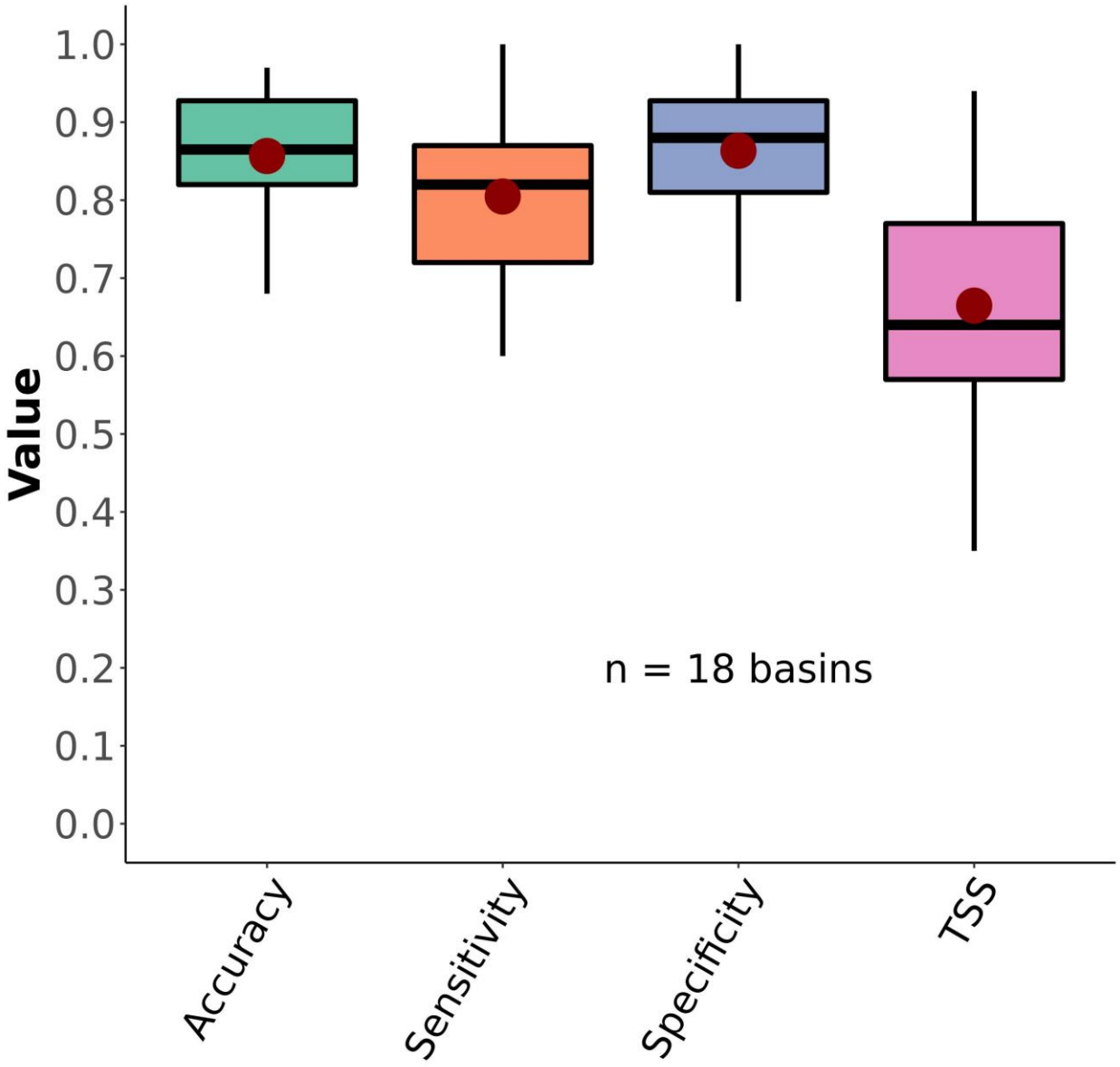

Figure S7: *Boxplots of regional ephemeral classification performance, by accuracy metric (section 3.2). Red dots correspond to the mean values. See Table S3 for metric definitions.*

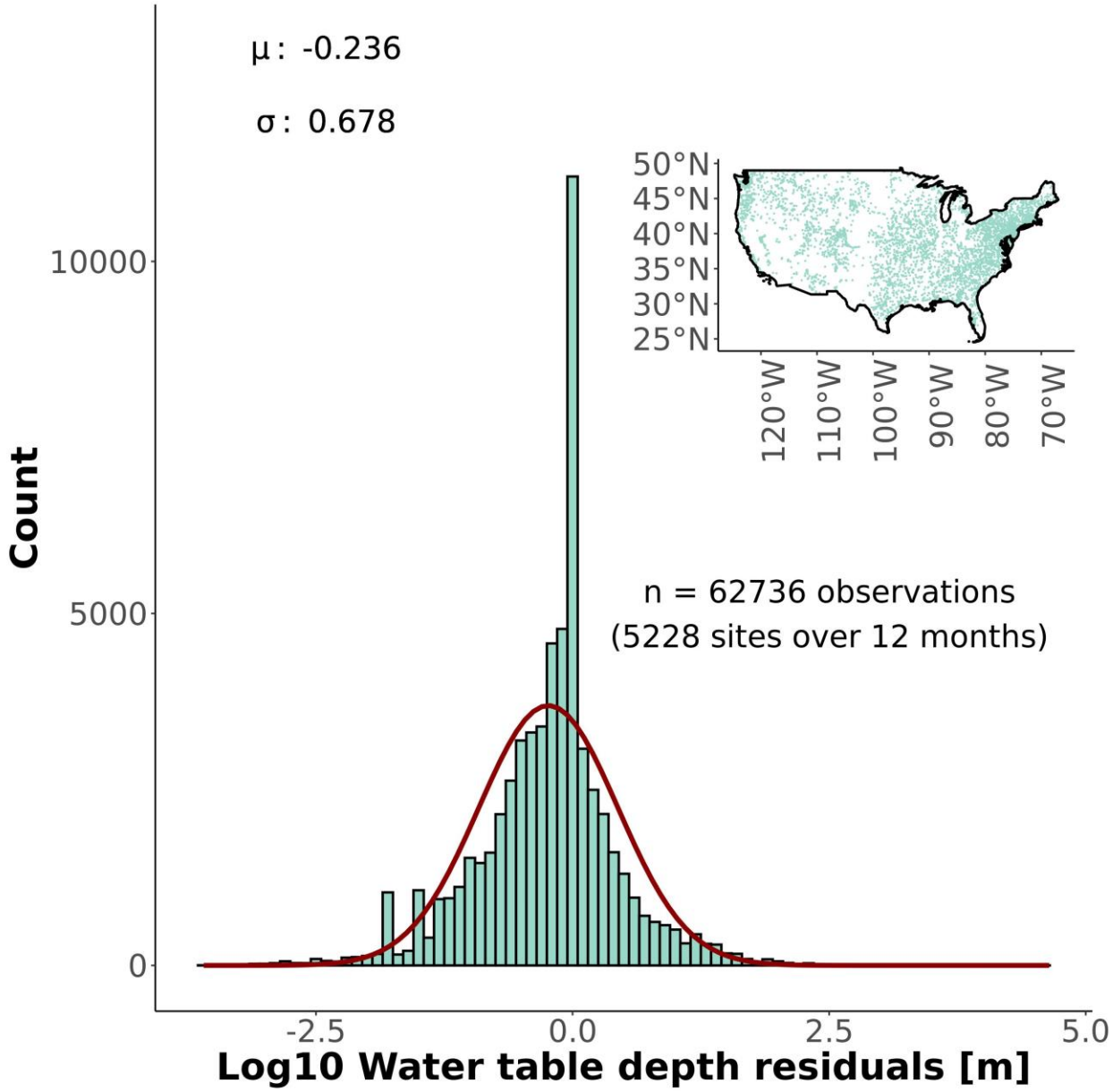

Figure S8: *Validation of mean monthly water table depths across the United States. Histogram of model log-residuals at groundwater wells and stream gauges (their distribution is mapped in the subplot). Wells are only those with at least 20 years of data and no deeper than 100m (19, 41) to calculate mean monthly well depths. Stream gauges are only those with at least 20 years of data and flowing 100% of the time. This means stream gauges represent perennial rivers with a relative water table depth of approximately 0m.*

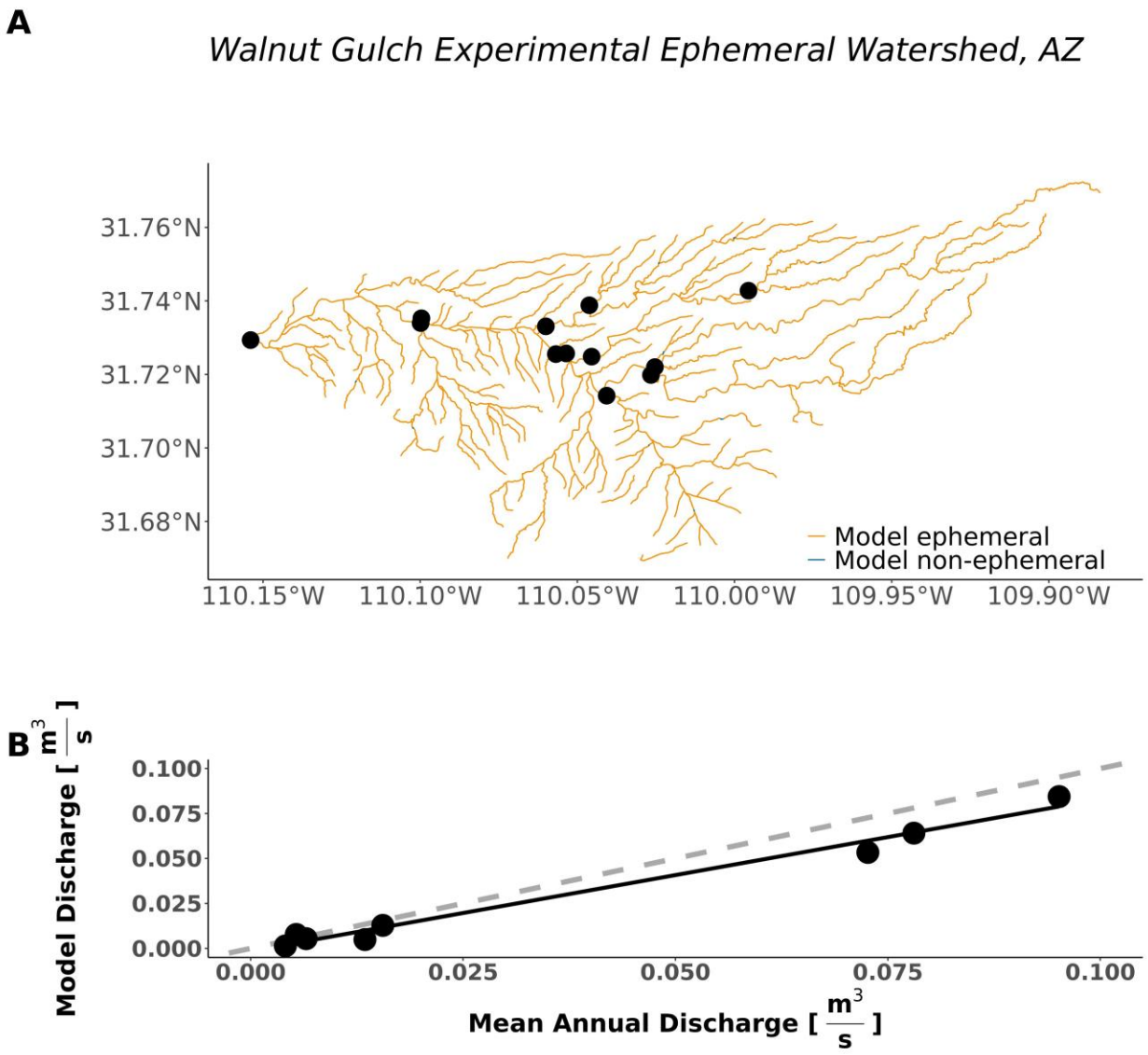

500

Figure S9: *Field-scale model performance in the ephemeral Walnut Gulch experimental watershed. (A) Map of the model classification, indicating that we successfully identify the entire watershed as ephemeral. (B) Validation of the mean annual discharge model at in-situ flumes within the watershed, which are also mapped in (A). For quality control, these flume data correspond to all sites whose reported drainage areas are within 20% of the drainage areas reported in the NHD-HR. Dashed grey line is the 1:1 line while the black line denotes the linear regression.*

505

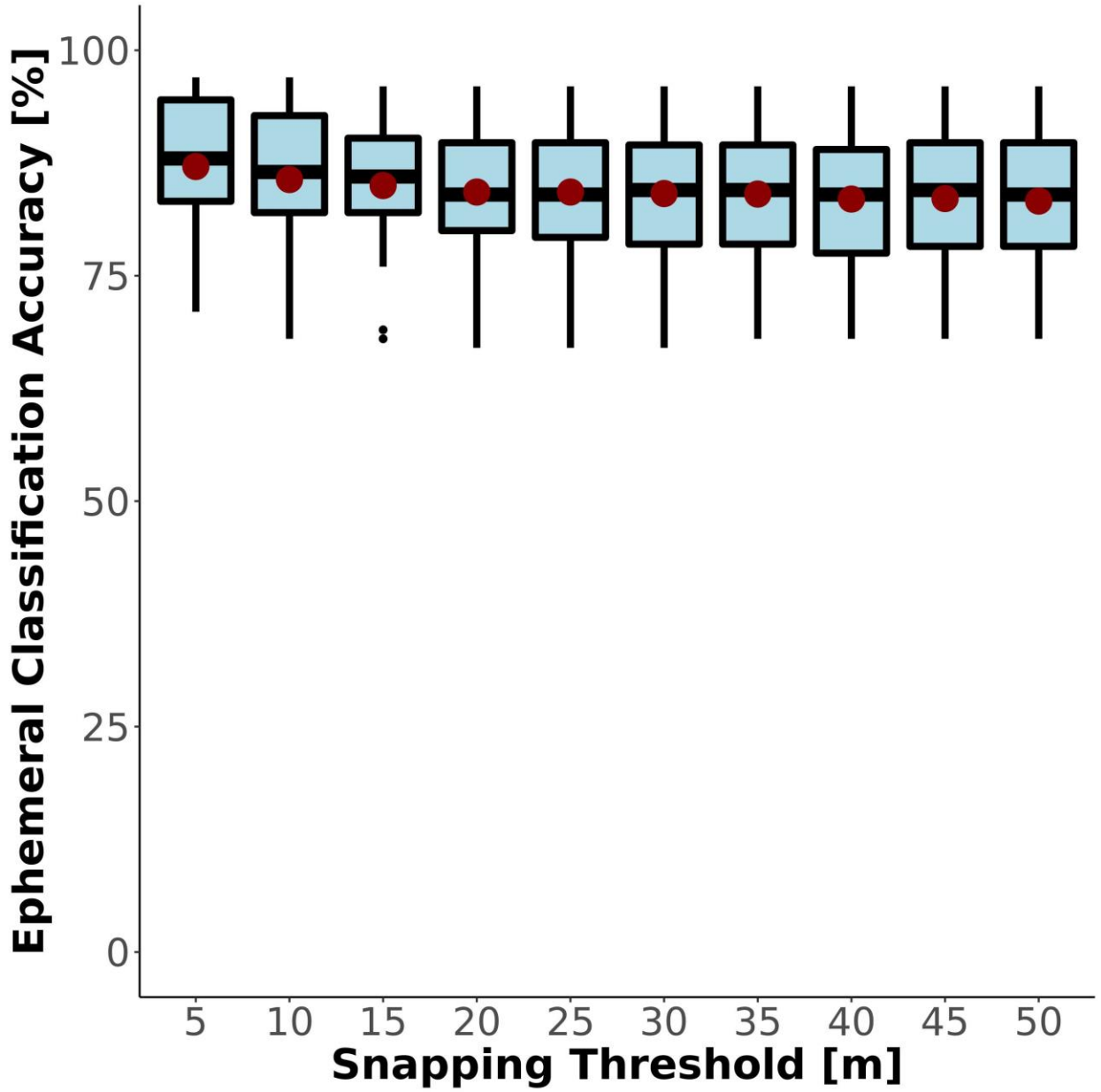

Figure S10: *: Sensitivity of ephemeral classification accuracy to the snapping threshold used to join in situ ephemerality data to the NHD-HR (section 3.3). Red points reflect the mean values.*

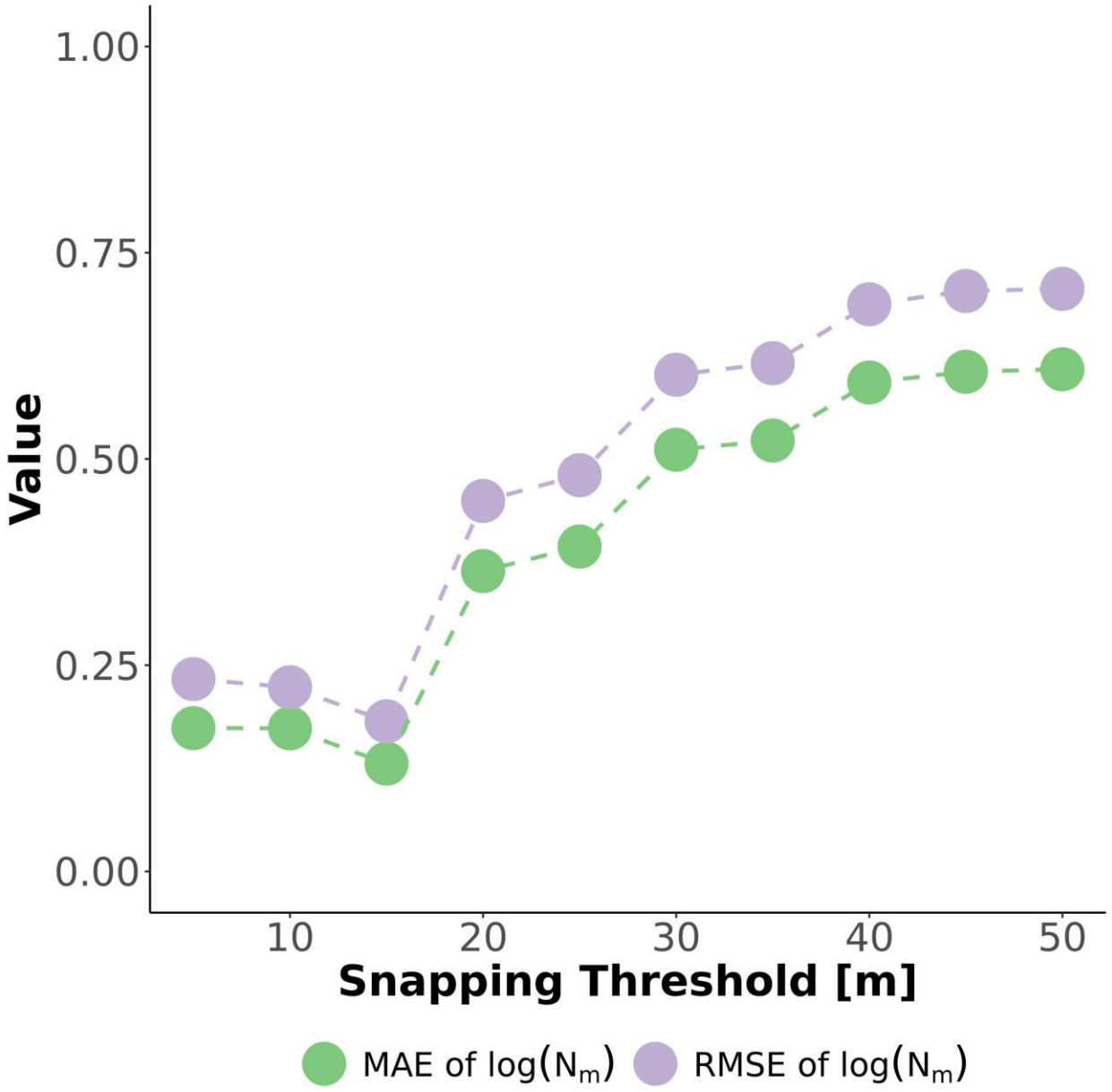

Figure S11: *: Using Horton stream order scaling to find a snapping threshold (section 3.3). Points and lines show how well the in situ ephemerality data (section 1.4) fits expected network scaling theory (equation S4) given a snapping threshold to the NHD-HR. Nm refers to the number of streams per order. Purple is the root mean square error (RMSE) and green is the mean absolute error (MAE) between the in situ Nm and the Nm predicted by Horton's laws. Metrics should be smallest when the data best match Horton's laws, indicating that we correctly capturing expected network patterns and are not miss-assigning field data to the wrong rivers.*

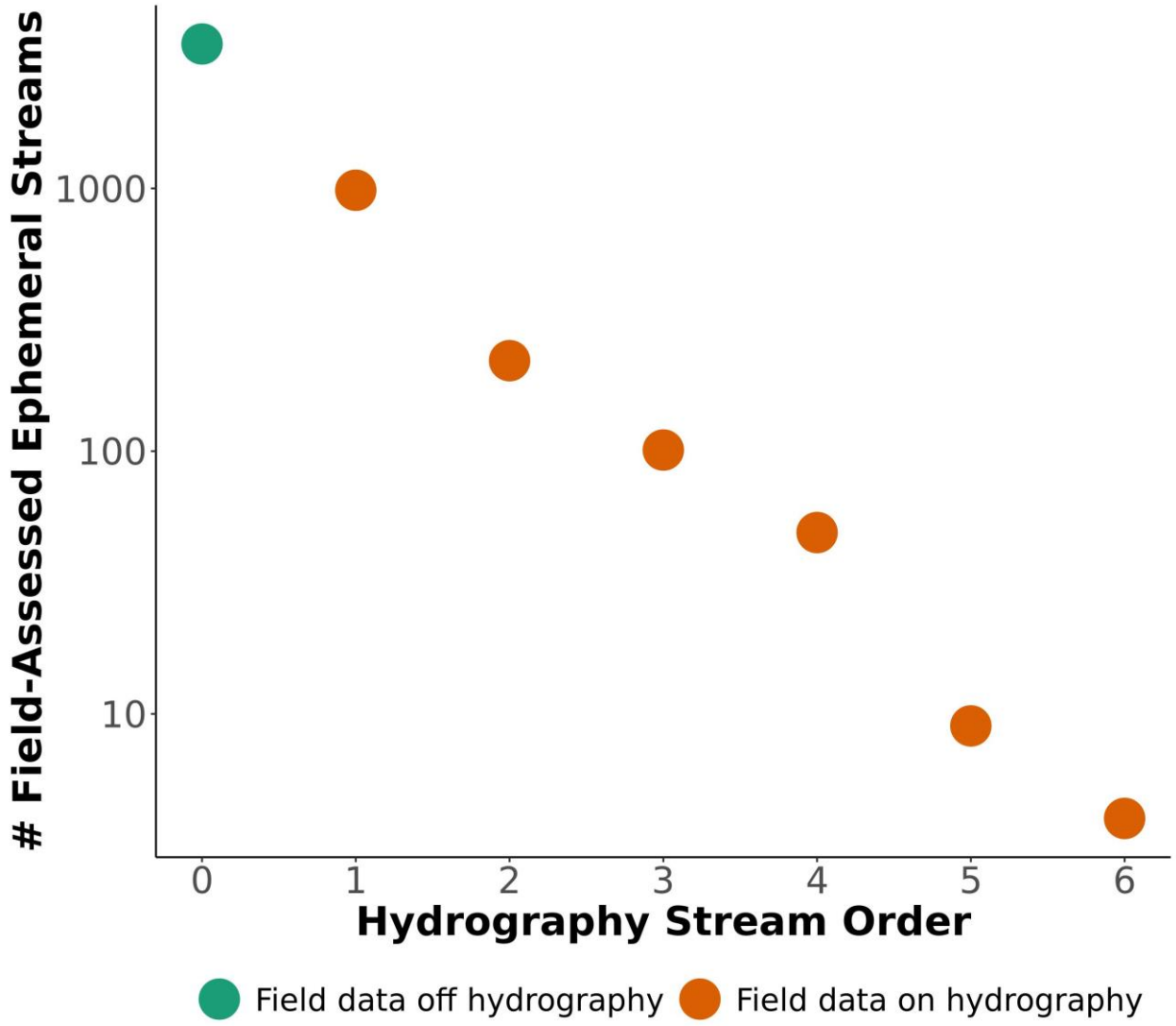

Figure S12: *: Scaling model for CONUS ephemeral stream network using in situ ephemerality data (section 1.4). Orange points represent ephemeral streams explicitly associated with NHD-HR reaches while the green point represents ephemeral streams implicitly represented in our headwater hydrography (see section 3.4).*

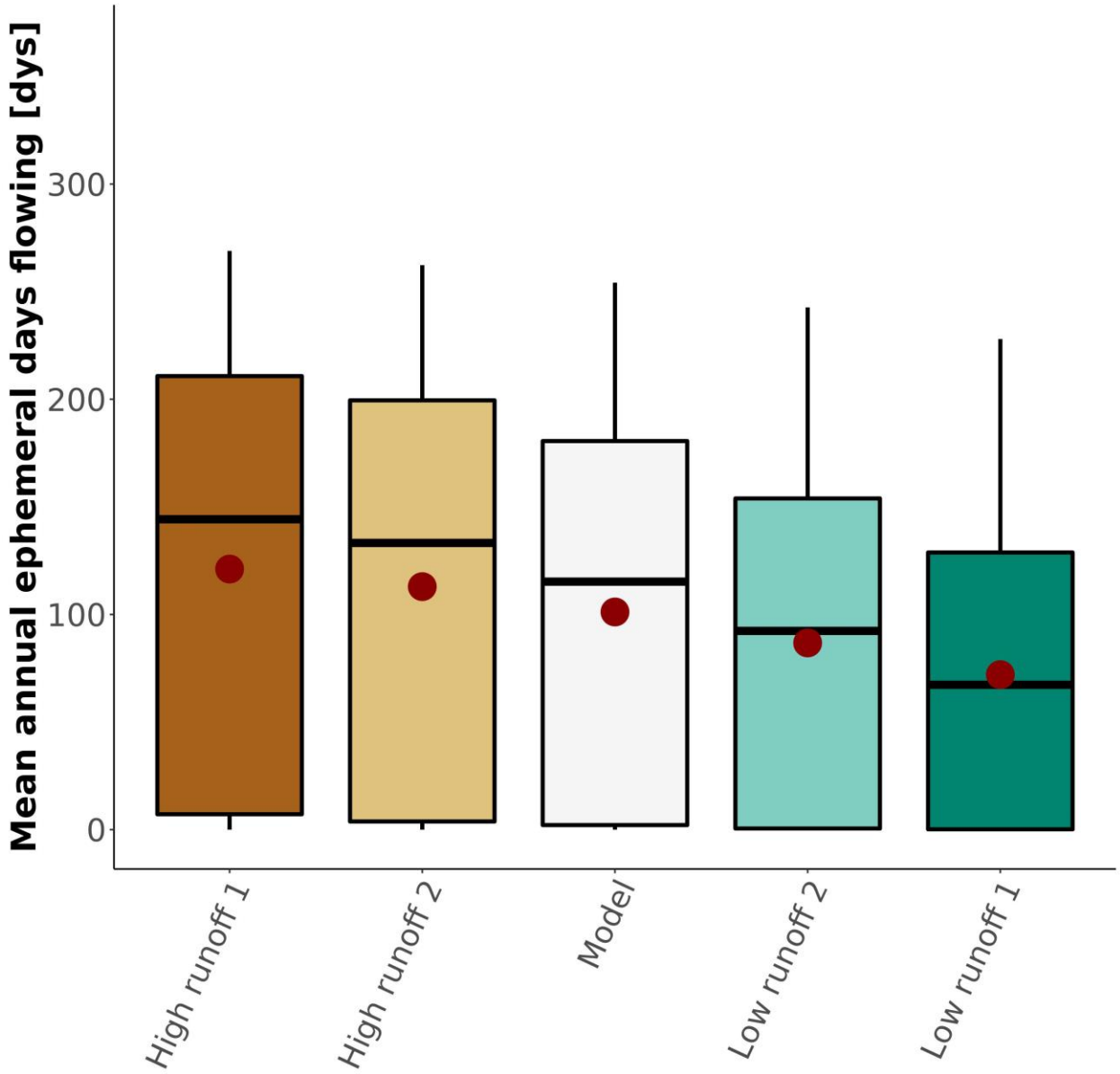

Figure S13: *: Sensitivity test for N_{flw} (section 4.2). The white boxplot is the distribution of the actual model results presented in the paper.*

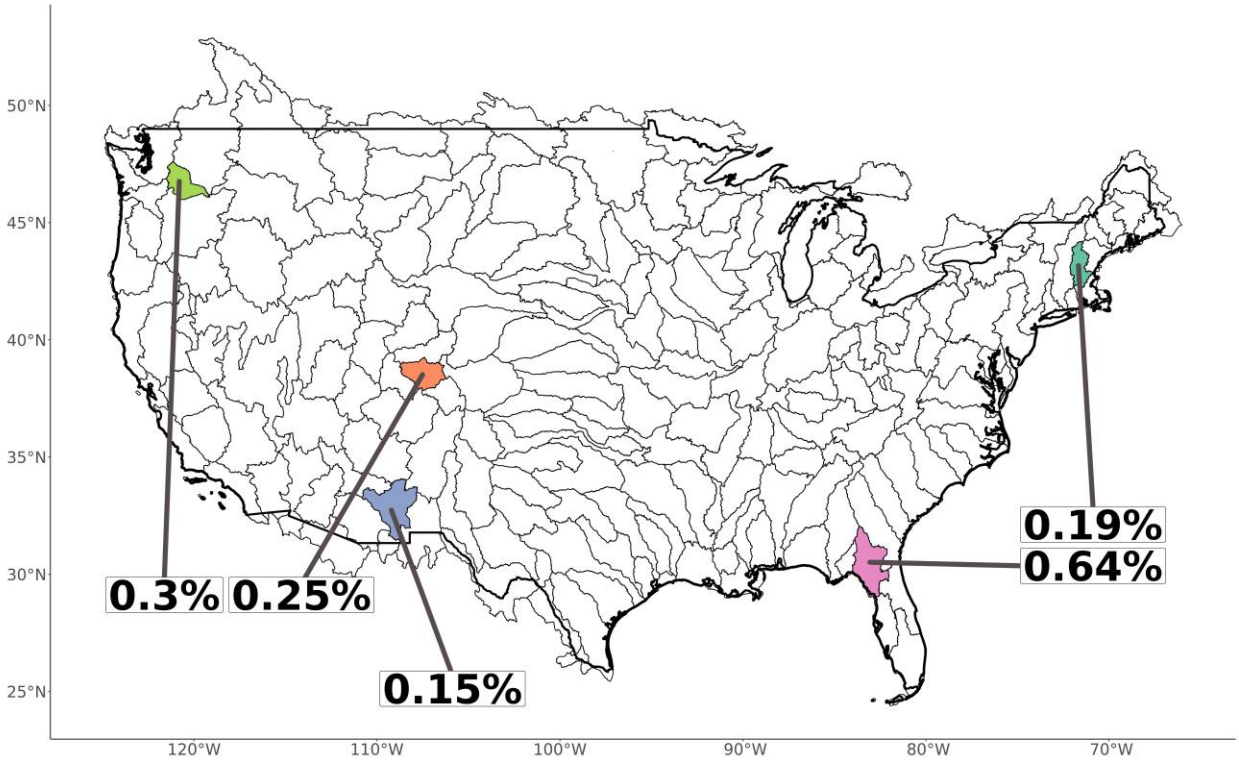

Figure S14: *: Uncertainty estimates (1 standard deviation from Monte Carlo simulations for our main metric: Eq. S1). We first parameterize uncertainty for both bankfull depth and water table depth (see Supplementary Materials S1). Then, we run 1,000 simulations of our model for each of the five basins. From those distributions, we use 1 standard deviation to characterize model uncertainty. All five uncertainties are < 1%.*

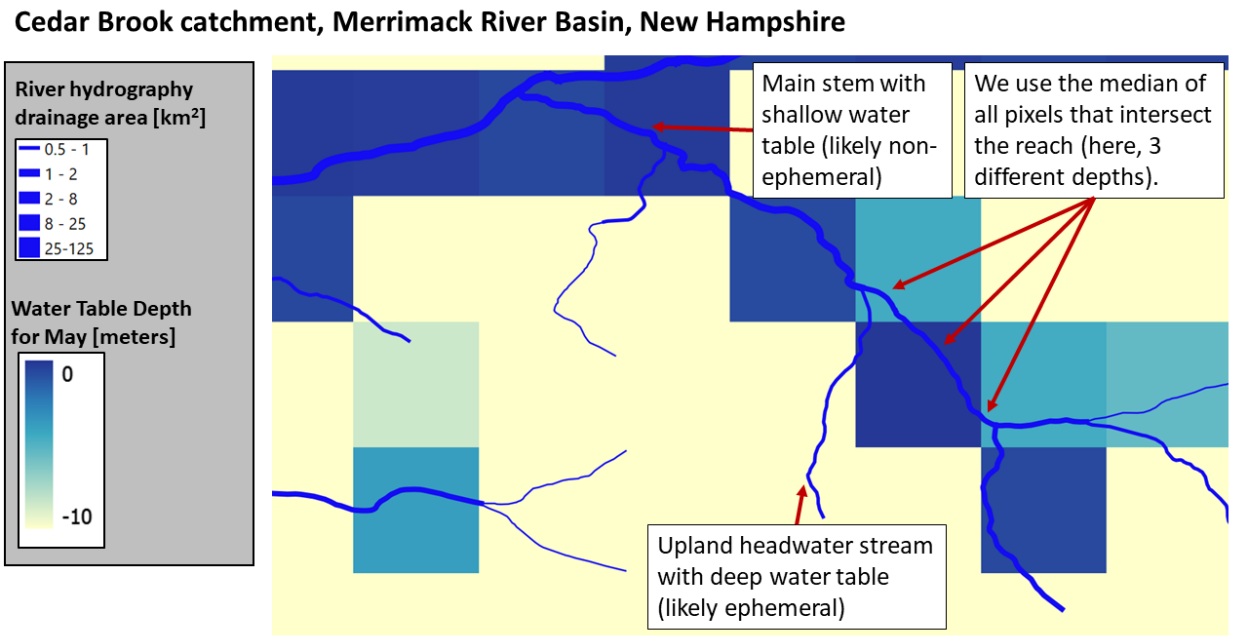

Figure S15: *Example of NHD-HR hydrography versus modeled water table depths for the Cedar Brook catchment in the Merrimack River basin (New Hampshire). After comparing water table depth to bankfull depth, we then route through the network to clean up impossible scenarios due to model artifacts. See Supplementary Materials for more details.*

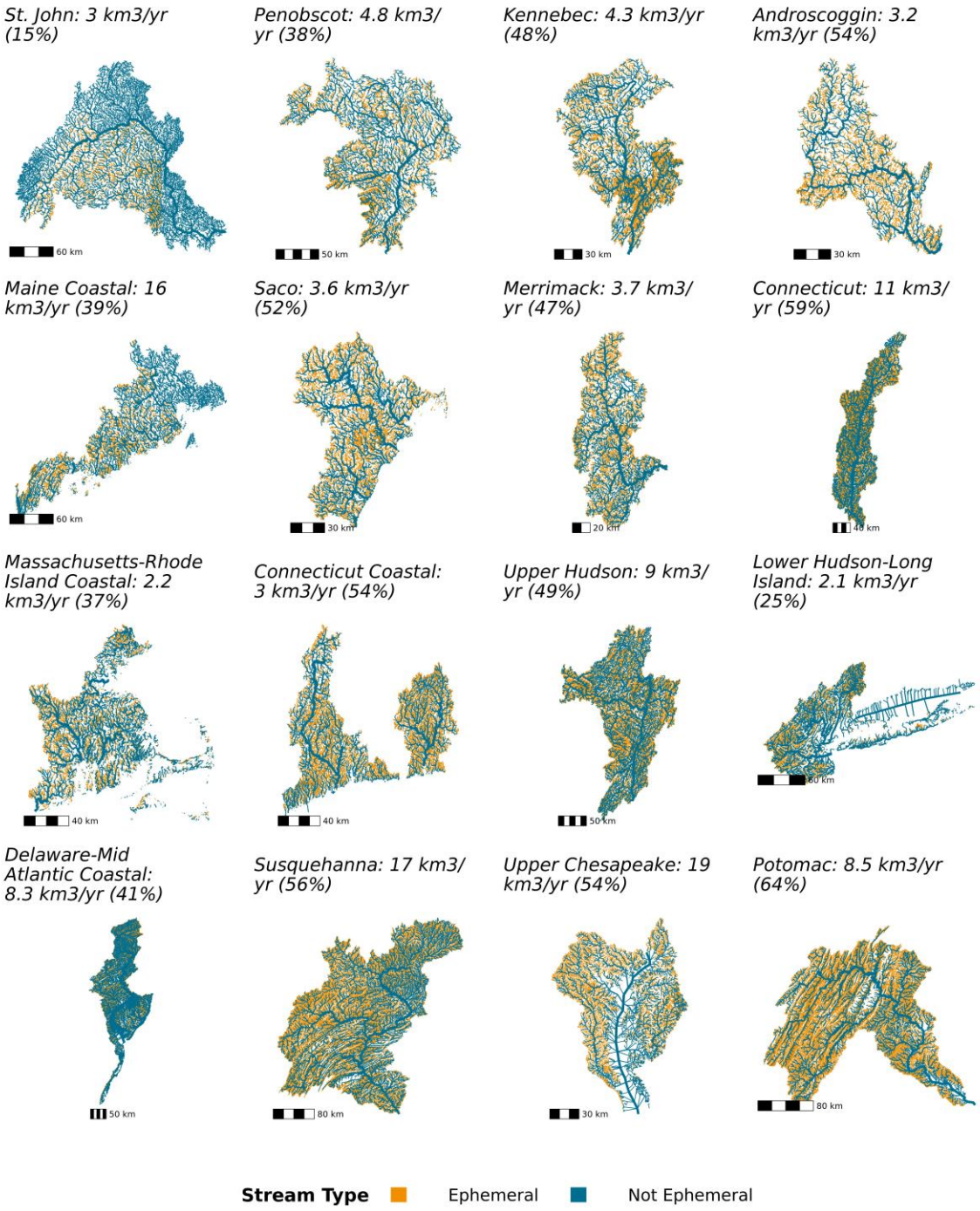

545

Figure S16: *Drainage network hydrographies 1-16 of 205. Sub-plot titles refer to the relative and absolute values of discharge exported from drainage networks that is ephemerally sourced (equation S1). Reach width corresponds to the size of the river (specifically, the logarithmic bins of discharge relative to map scale). Note that foreign streams are mapped as 'not ephemeral' in these plots for visualization's sake.*

550

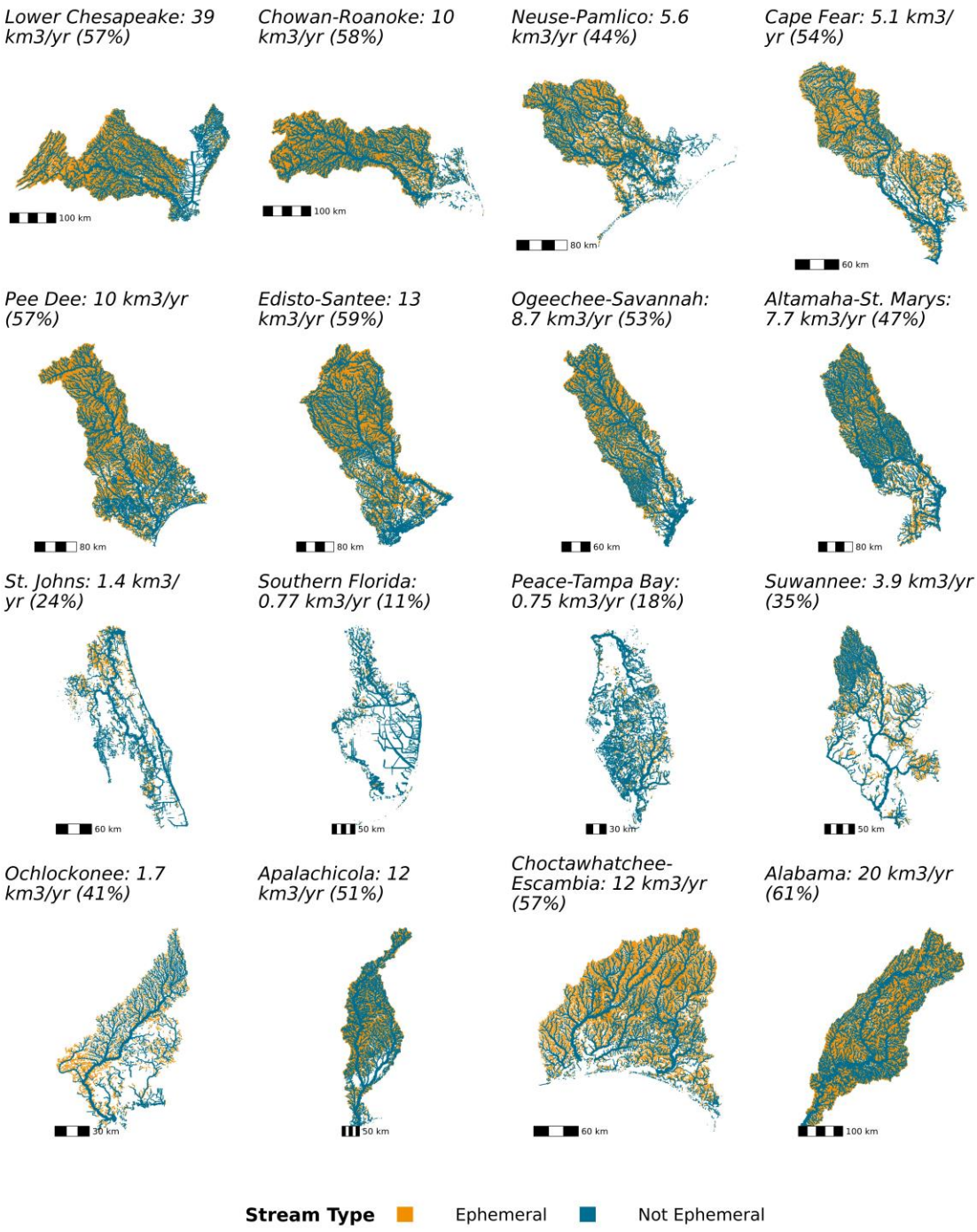

Figure S17: *Drainage network hydrographies 17-32 of 205. Sub-plot titles refer to the relative and absolute values of discharge exported from drainage networks that is ephemerally sourced (equation S1). Reach width corresponds to the size of the river (specifically, the logarithmic bins of discharge relative to map scale). Note that foreign streams are mapped as 'not ephemeral' in these plots for visualization's sake.*

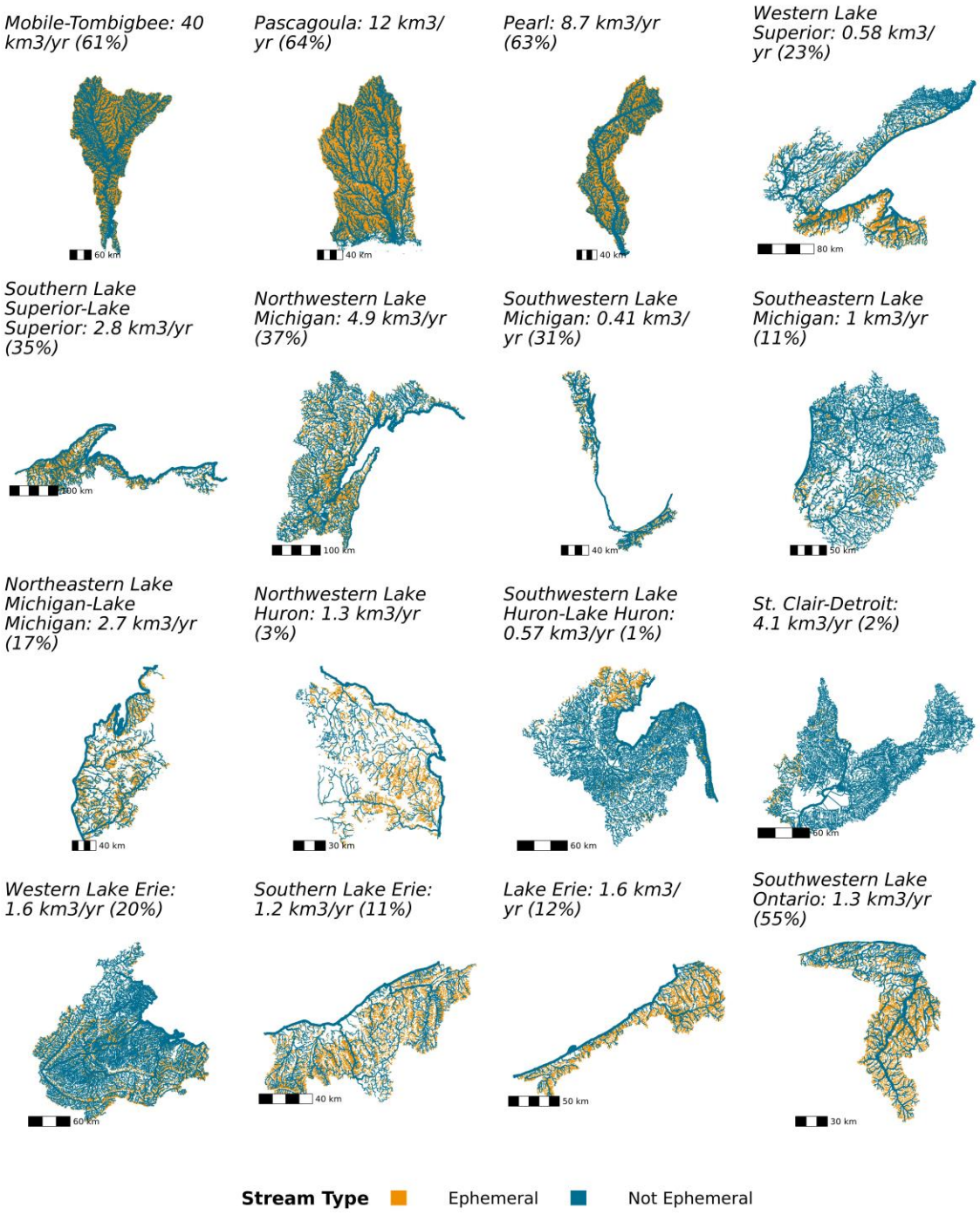

Figure S18: *Drainage network hydrographies 33-48 of 205. Sub-plot titles refer to the relative and absolute values of discharge exported from drainage networks that is ephemerally sourced (equation S1). Reach width corresponds to the size of the river (specifically, the logarithmic bins of discharge relative to map scale). Note that foreign streams are mapped as 'not ephemeral' in these plots for visualization's sake.*

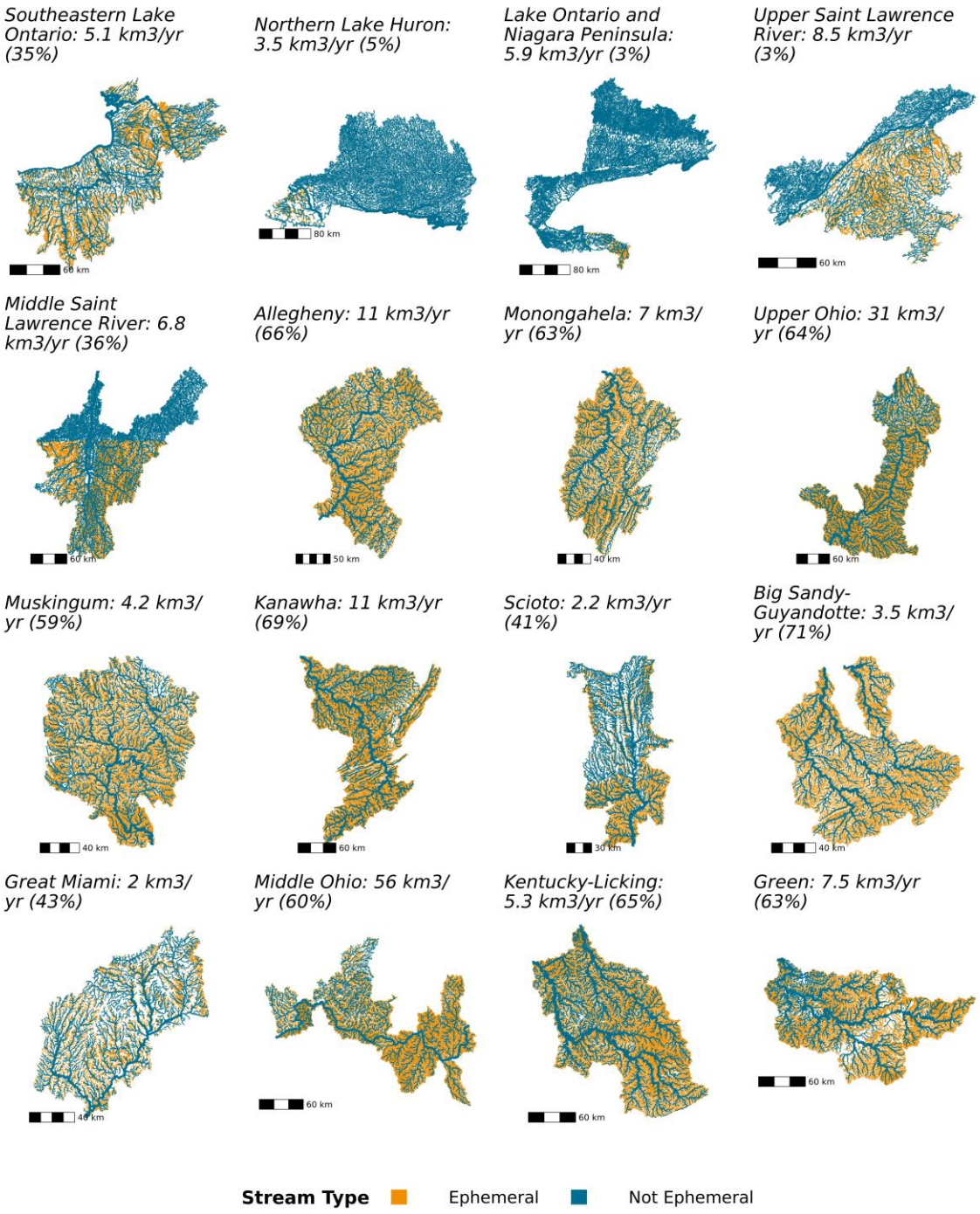

Figure S19: *Drainage network hydrographies 49-64 of 205. Sub-plot titles refer to the relative and absolute values of discharge exported from drainage networks that is ephemerally sourced (equation S1). Reach width corresponds to the size of the river (specifically, the logarithmic bins of discharge relative to map scale). Note that foreign streams are mapped as 'not ephemeral' in these plots for visualization's sake.*

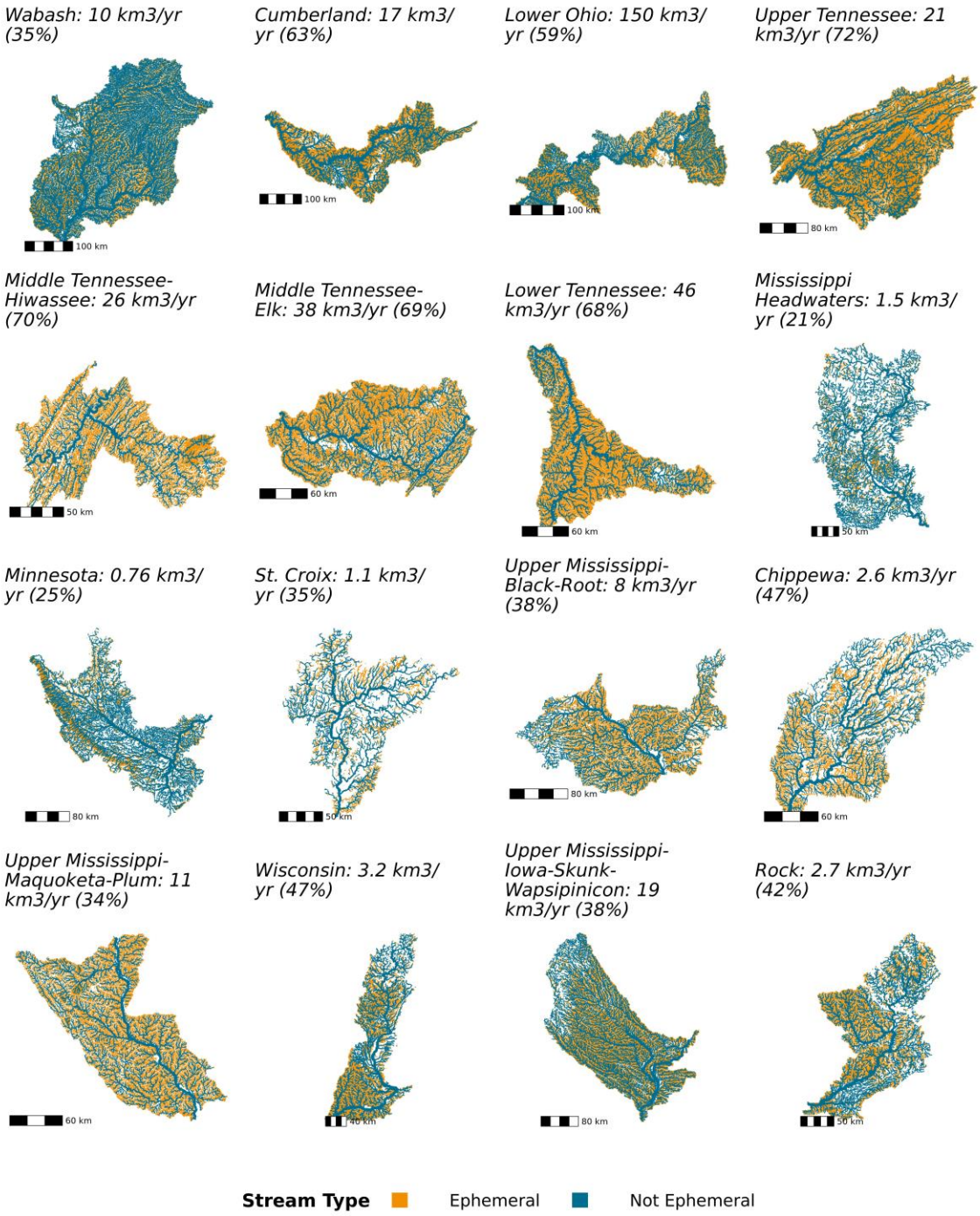

Figure S20: *Drainage network hydrographies 65-80 of 205. Sub-plot titles refer to the relative and absolute values of discharge exported from drainage networks that is ephemerally sourced (equation S1). Reach width corresponds to the size of the river (specifically, the logarithmic bins of discharge relative to map scale). Note that foreign streams are mapped as 'not ephemeral' in these plots for visualization's sake.*

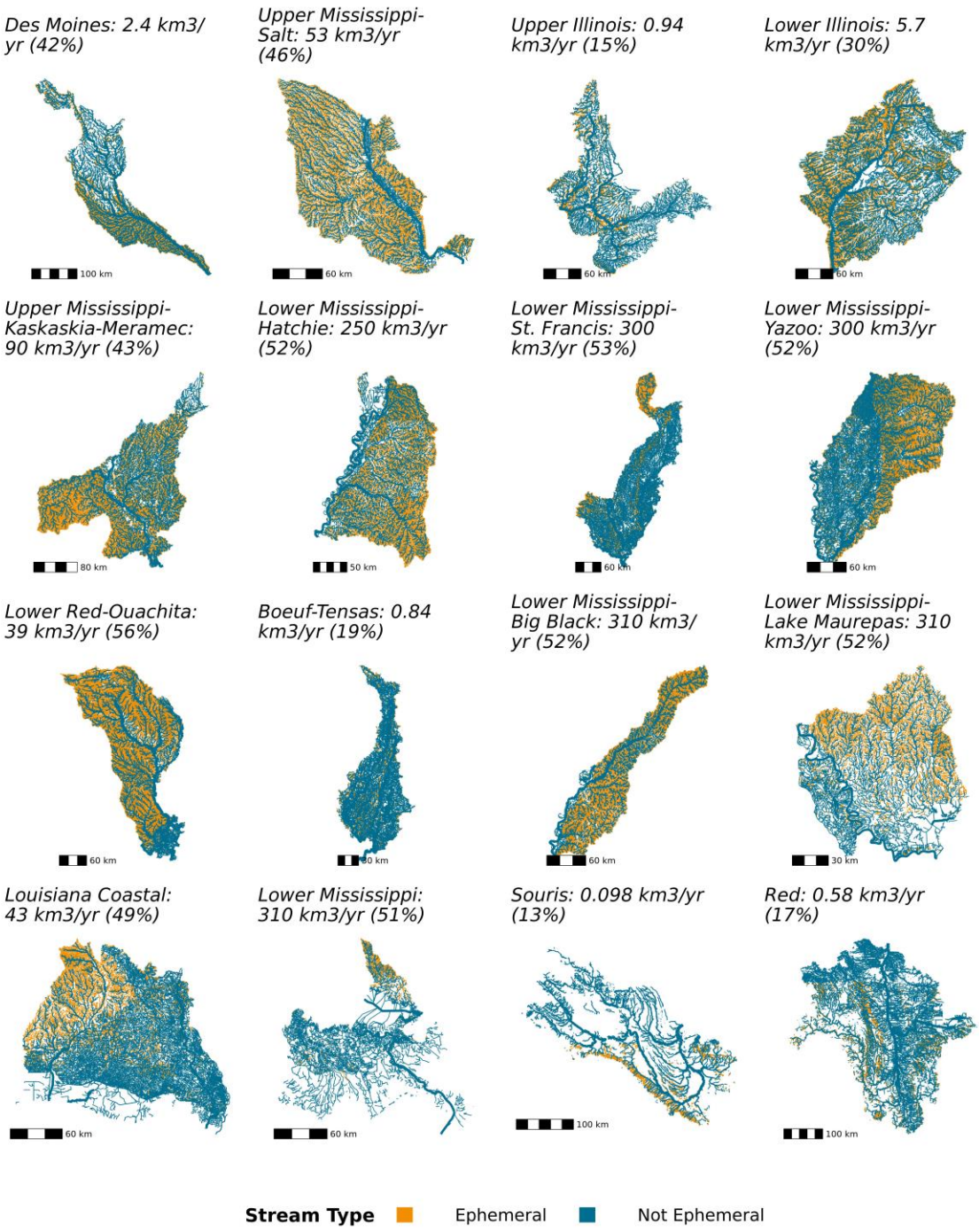

Figure S21: *Drainage network hydrographies 81-96 of 205. Sub-plot titles refer to the relative and absolute values of discharge exported from drainage networks that is ephemerally sourced (equation S1). Reach width corresponds to the size of the river (specifically, the logarithmic bins of discharge relative to map scale). Note that foreign streams are mapped as 'not ephemeral' in these plots for visualization's sake.*

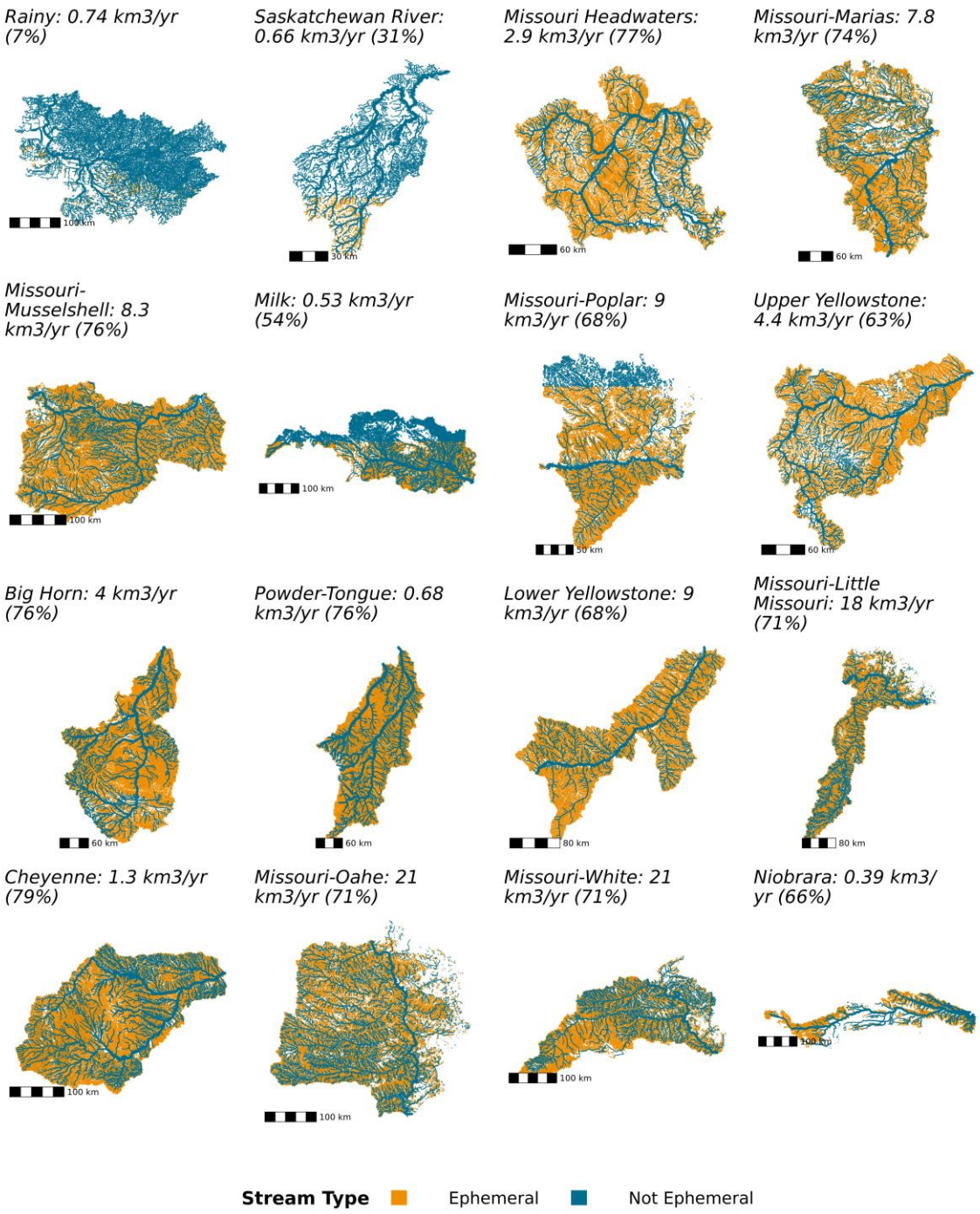

Figure S22: *Drainage network hydrographies 97-112 of 205. Sub-plot titles refer to the relative and absolute values of discharge exported from drainage networks that is ephemerally sourced (equation S1). Reach width corresponds to the size of the river (specifically, the logarithmic bins of discharge relative to map scale). Note that foreign streams are mapped as 'not ephemeral' in these plots for visualization's sake.*

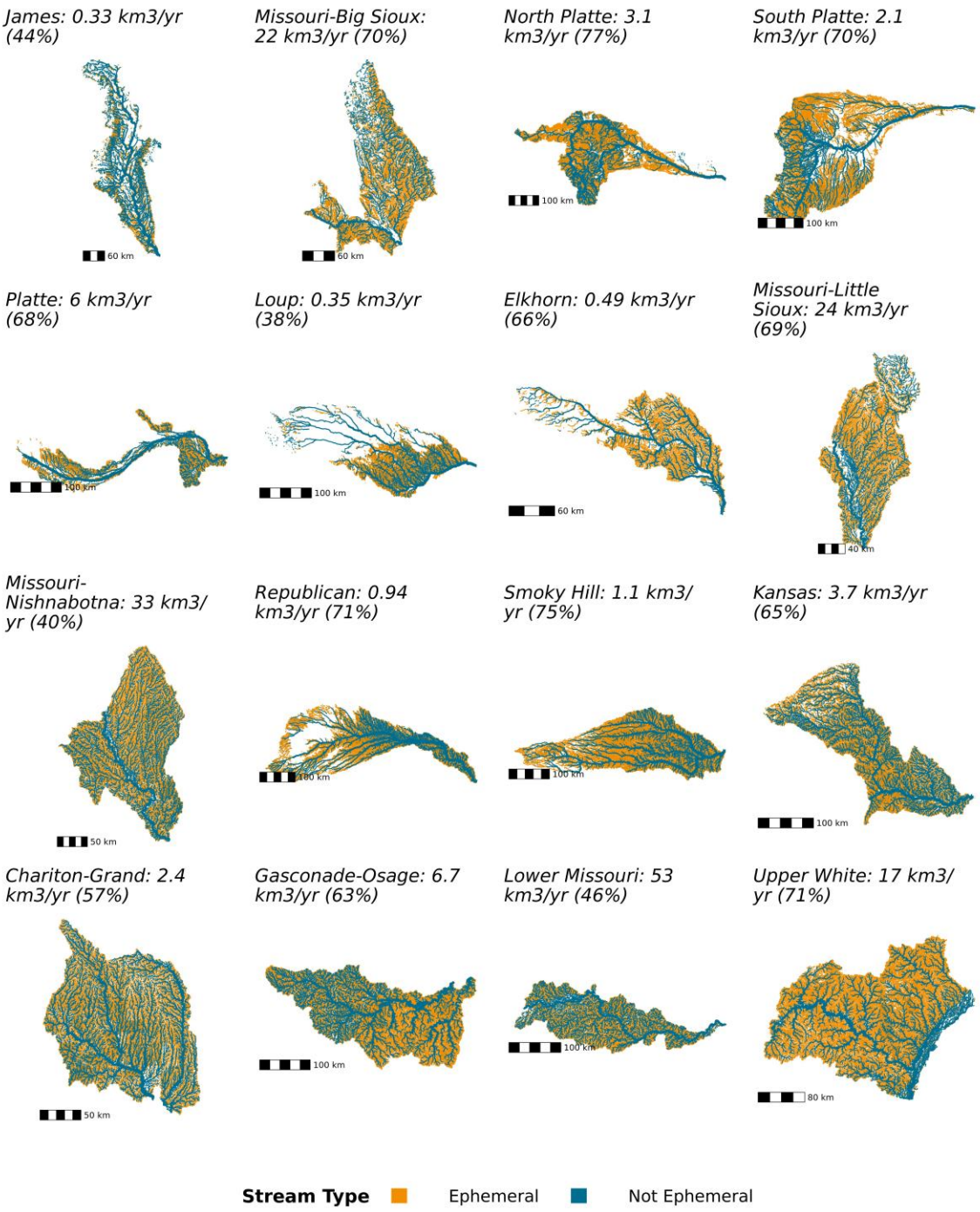

Figure S23: *Drainage network hydrographies 113-128 of 205. Sub-plot titles refer to the relative and absolute values of discharge exported from drainage networks that is ephemerally sourced (equation S1). Reach width corresponds to the size of the river (specifically, the logarithmic bins of discharge relative to map scale). Note that foreign streams are mapped as 'not ephemeral' in these plots for visualization's sake.*

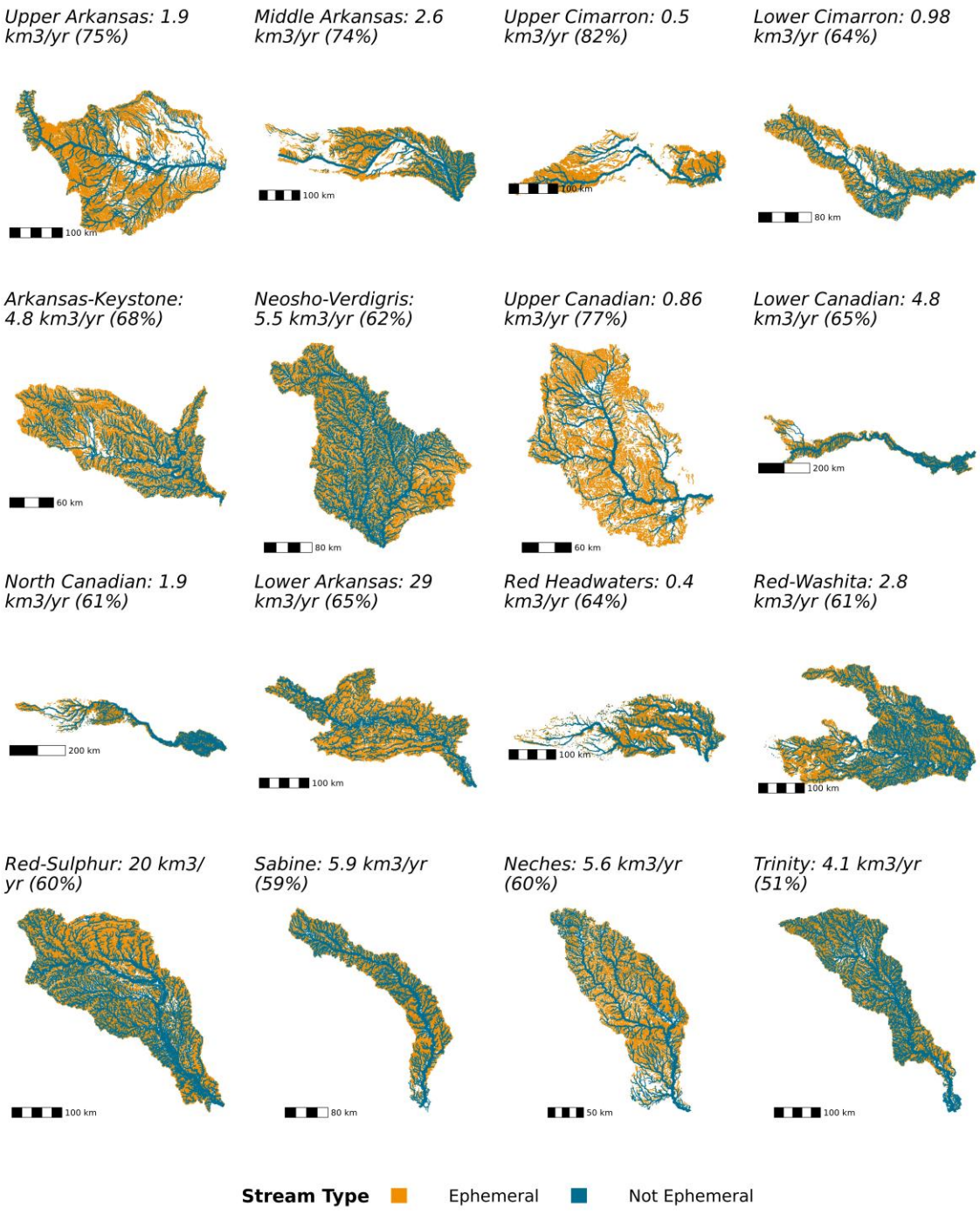

Figure S24: *Drainage network hydrographies 129-144 of 205. Sub-plot titles refer to the relative and absolute values of discharge exported from drainage networks that is ephemerally sourced (equation S1). Reach width corresponds to the size of the river (specifically, the logarithmic bins of discharge relative to map scale). Note that foreign streams are mapped as 'not ephemeral' in these plots for visualization's sake.*

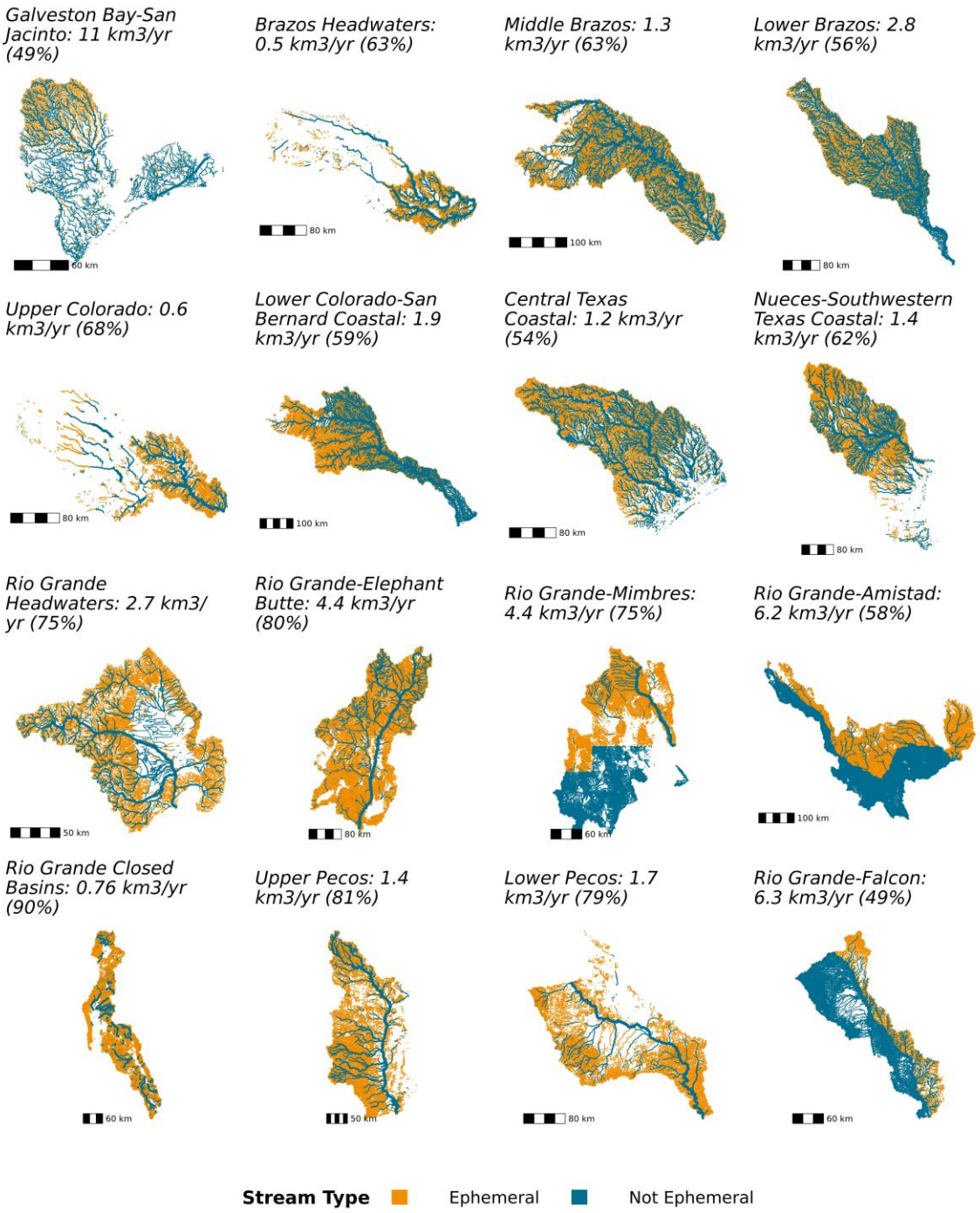

600 ***Figure S25:*** *Drainage network hydrographies 145-160 of 205. Sub-plot titles refer to the relative and absolute values of discharge exported from drainage networks that is ephemerally sourced (equation S1). Reach width corresponds to the size of the river (specifically, the logarithmic bins of discharge relative to map scale). Note that foreign streams are mapped as 'not ephemeral' in these plots for visualization's sake.*

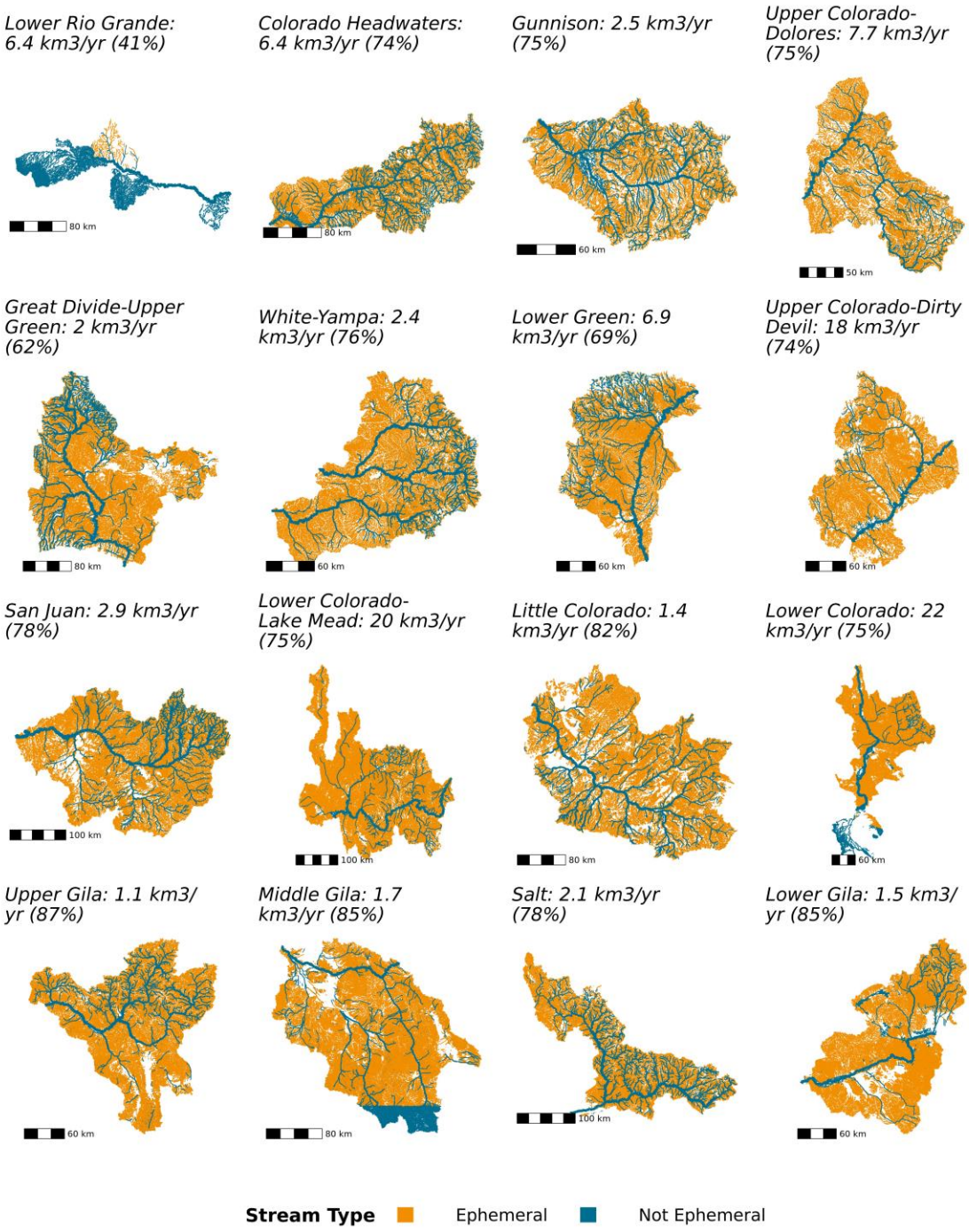

Figure S26: *Drainage network hydrographies 161-176 of 205. Sub-plot titles refer to the relative and absolute values of discharge exported from drainage networks that is ephemerally sourced (equation S1). Reach width corresponds to the size of the river (specifically, the logarithmic bins of discharge relative to map scale). Note that foreign streams are mapped as 'not ephemeral' in these plots for visualization's sake.*

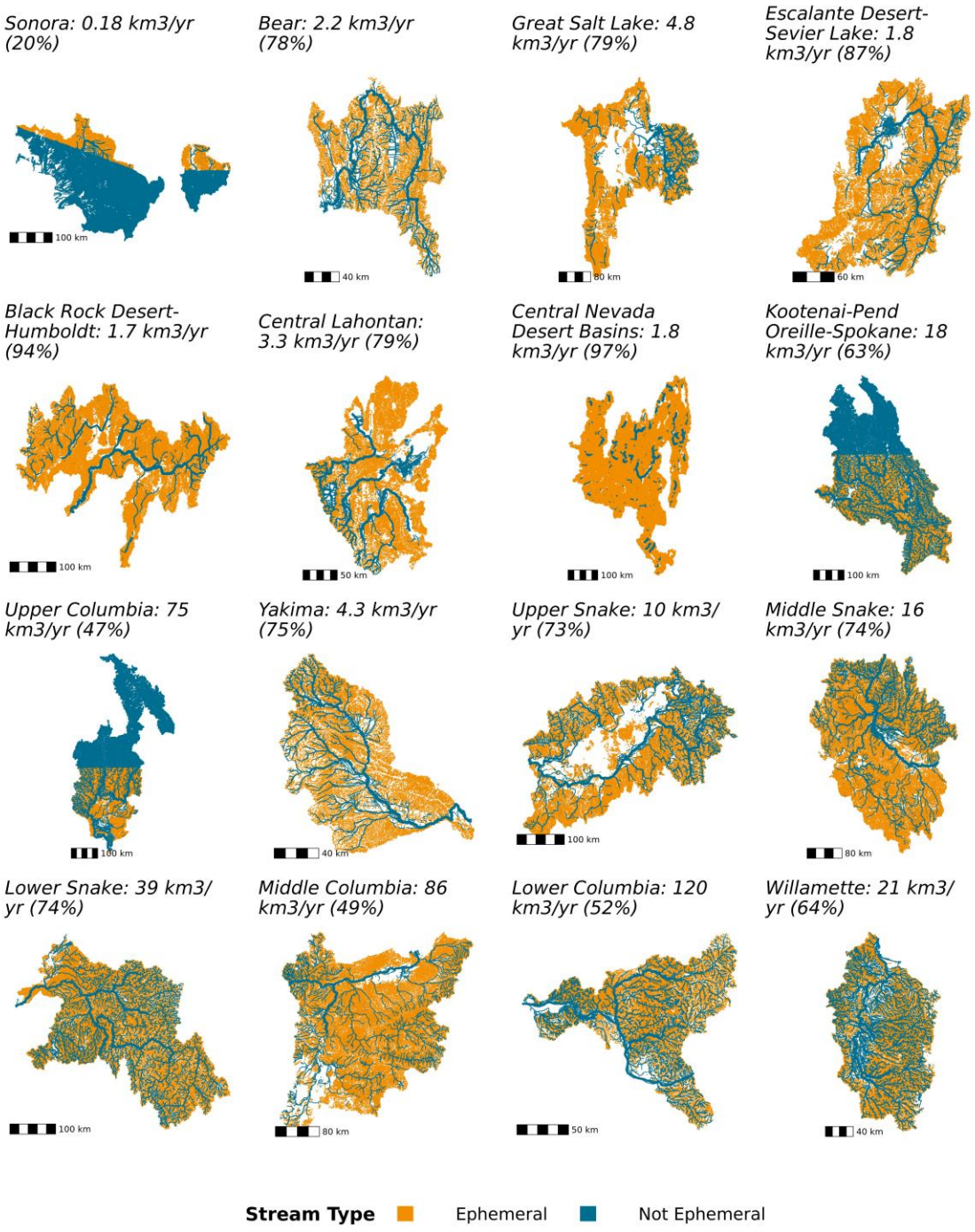

Figure S27: *Drainage network hydrographies 177-192 of 205. Sub-plot titles refer to the relative and absolute values of discharge exported from drainage networks that is ephemerally sourced (equation S1). Reach width corresponds to the size of the river (specifically, the logarithmic bins of discharge relative to map scale). Note that foreign streams are mapped as 'not ephemeral' in these plots for visualization's sake.*

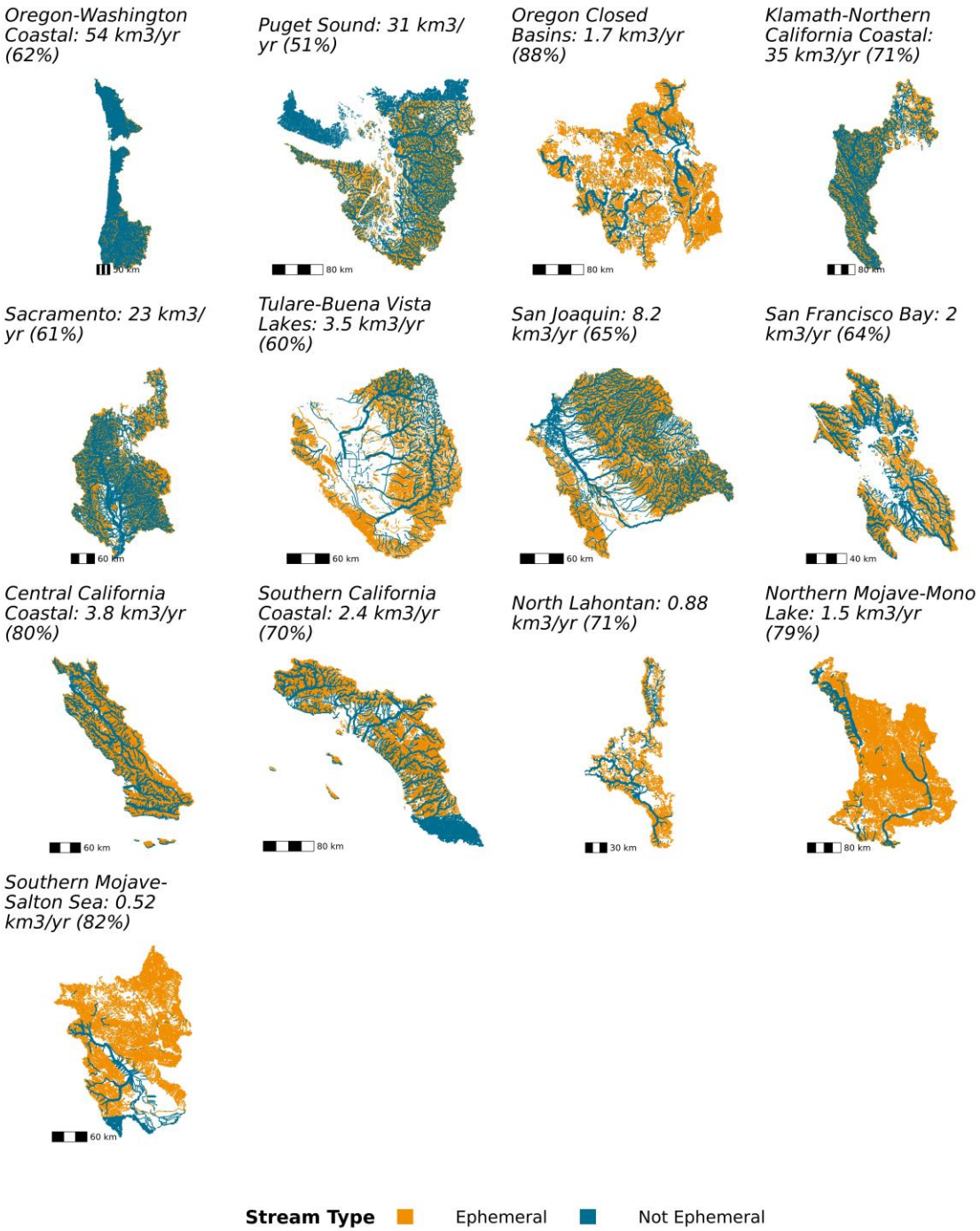

Figure S28: *Drainage network hydrographies 193-205 of 205. Sub-plot titles refer to the relative and absolute values of discharge exported from drainage networks that is ephemerally sourced (equation S1). Reach width corresponds to the size of the river (specifically, the logarithmic bins of discharge relative to map scale). Note that foreign streams are mapped as 'not ephemeral' in these plots for visualization's sake.*

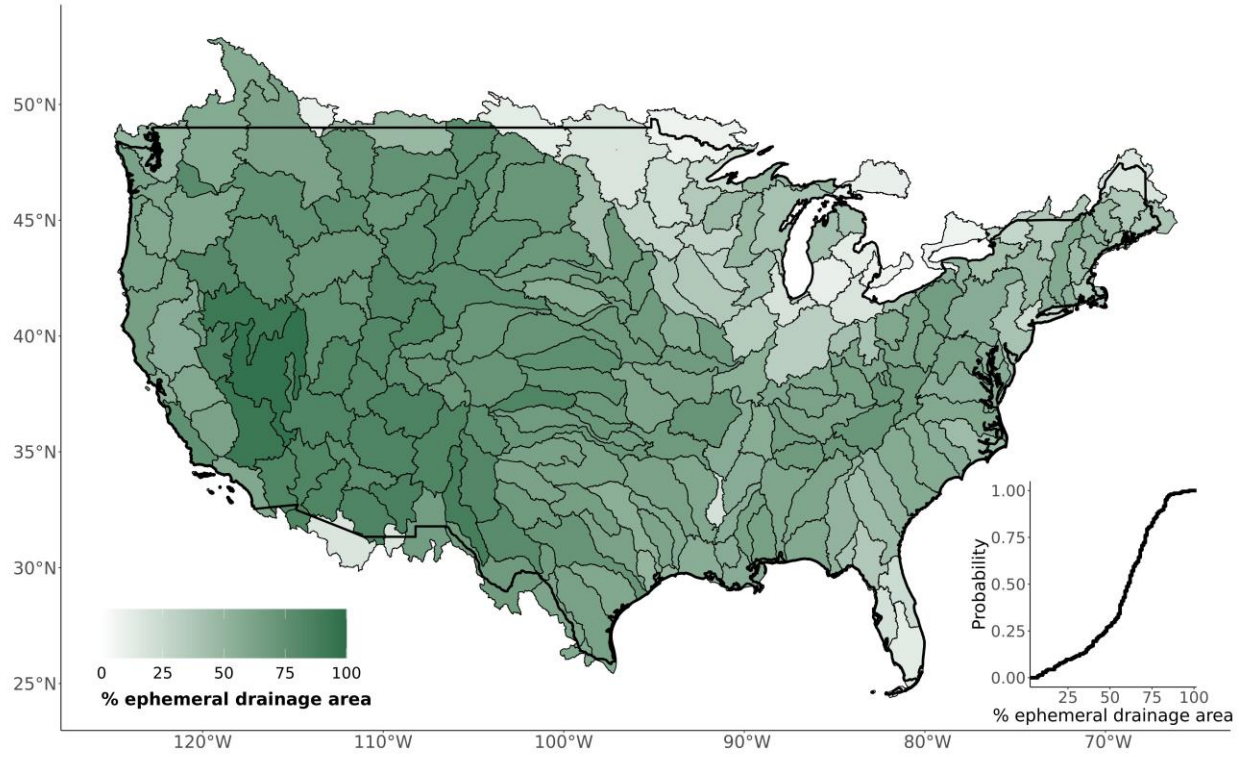

Figure S29: *Contiguous United States map of the percent of upstream drainage area that contributes to ephemeral streams (equation S2).*

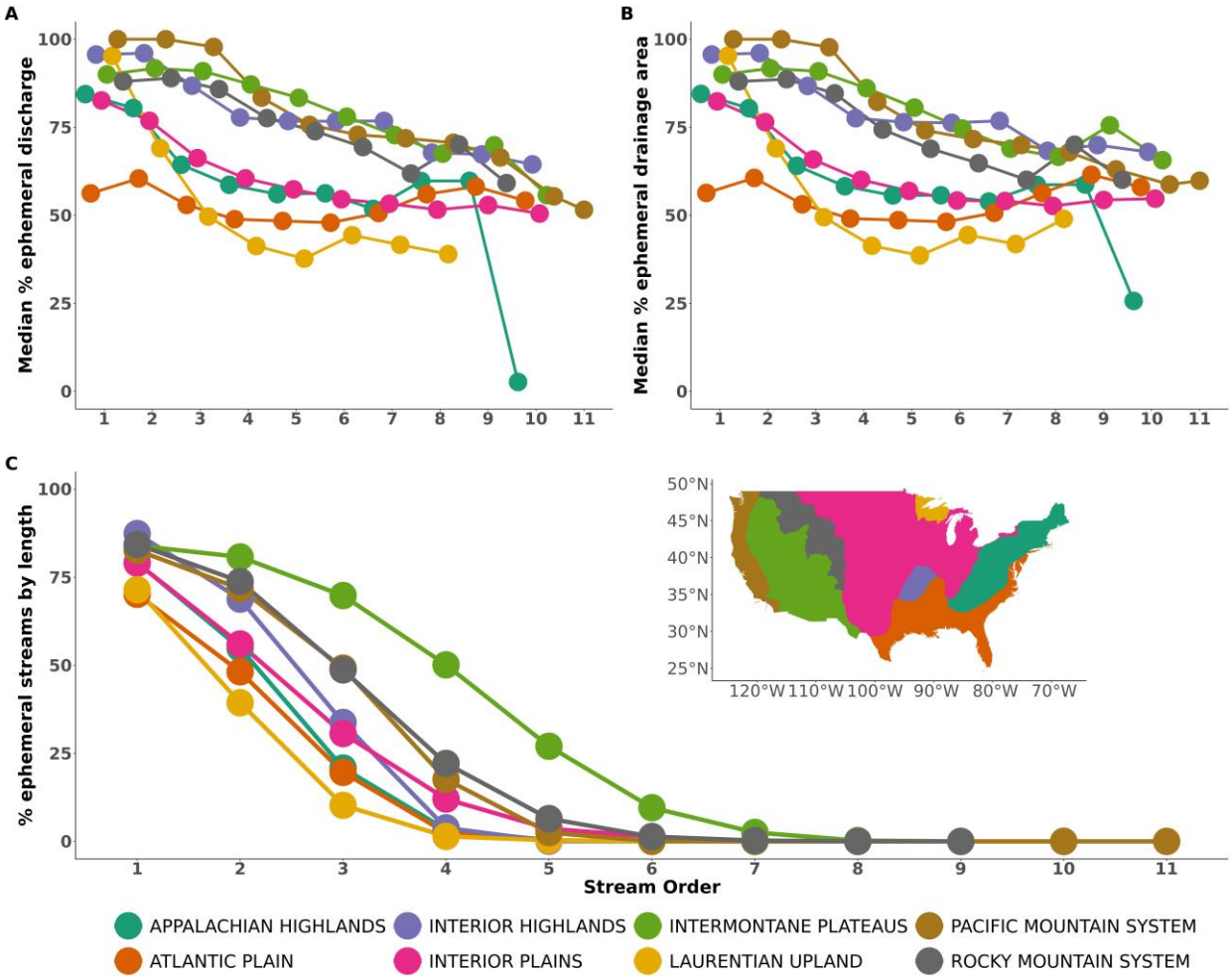

Figure S30: *Ephemeral contributions to United States drainage networks, separated by stream order and physiographic region (Fenneman & Johnson, 1946). Points correspond to the average across all basins predominately in each physiographic region. Note there is a single 10th order basin in the Appalachian Highlands, which causes the outlier value.*

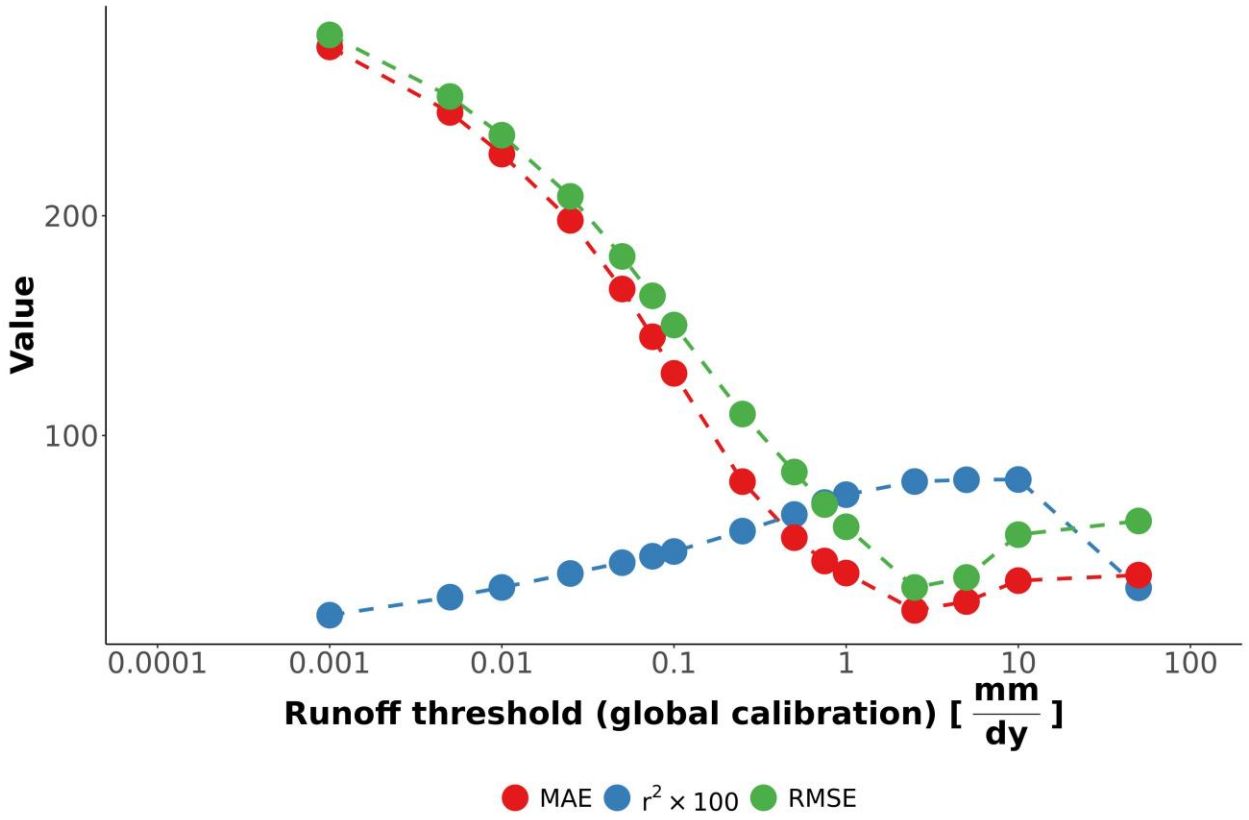

Figure S31: *Determining an operational streamflow definition (i_{min}) using the available N_{flw} data (section 4.2). MAE is mean absolute error, RMSE is root mean square error, and r2 is the coefficient of determination.*

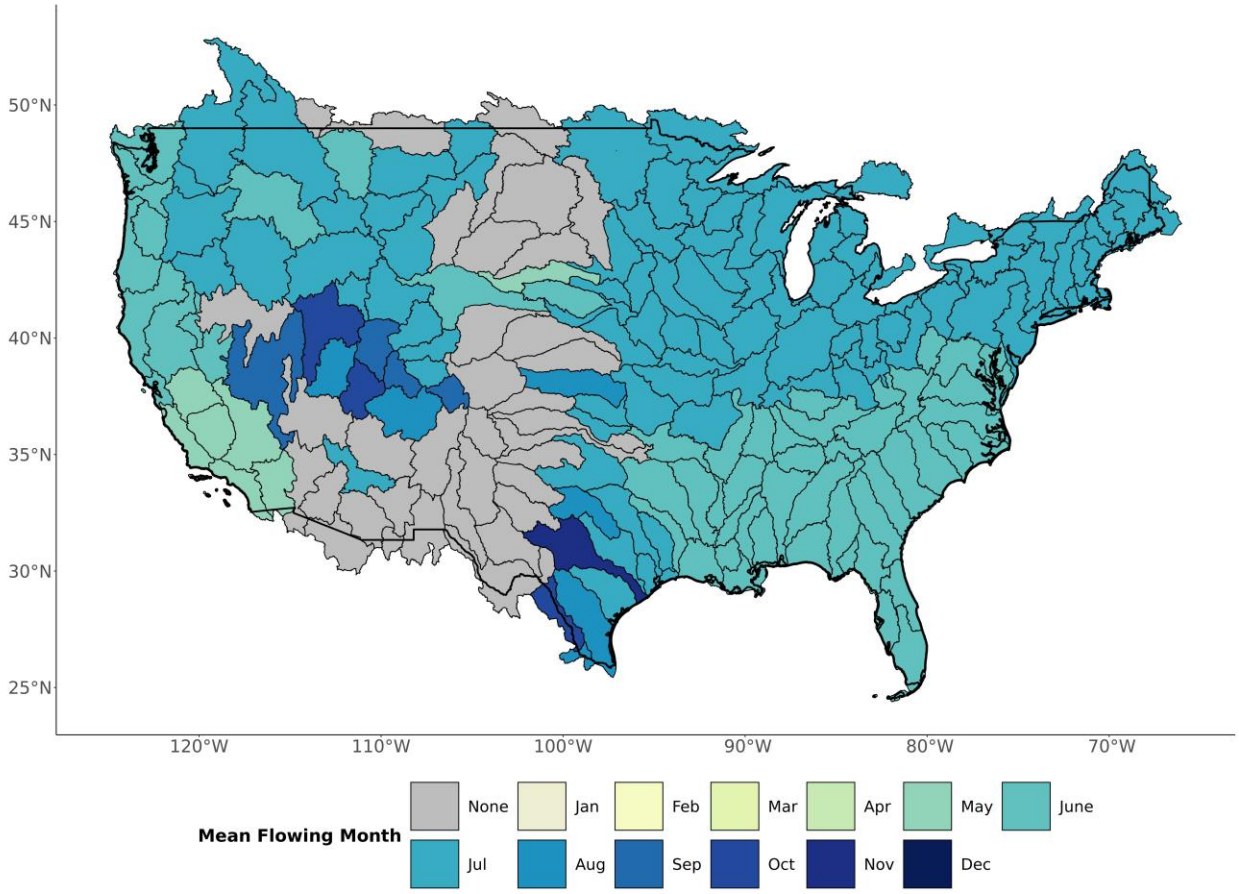

Figure S32: *Mean flowing month for ephemeral streams in each CONUS basin. Basins classed as 'None' do not flow frequently enough for a mean flowing month.*

Supplementary Tables

Table S1: Summary of models and data used to drive our model and generate our results. In situ data for validation is described in sections 1.4 and 4.1.

Variable	**Dataset Name**	**Spatial Resolution**	**Temporal Resolution**	**Years captured**	**Reference**
Hydrography	USGS National Hydrography Dataset High Resolution (NHD-HR)	1:24,000	-	Long-term	(*22*)
Discharge	USGS Mean Annual Discharge Model	1:24,000	Year	1970-2000	(*22*)
Water Table Depth	Fan Global Soil Hydrology Model	30”	Month	2004-2014	(*19*, *20*)
Precipitation	CPC Unified Gauge-Based Daily Precipitation Model	0.25’	Day	1980-2006	(*42*, *75*)
Runoff	USGS Runoff Data	USGS level 4 basins	Year	varies (from 1901-2021)	(*43*)

Table S2: In situ measurements of mean annual number of flowing days for ephemeral streams

Drainage Basin	Observed Nflw [dys]	Number Sample Years	Number Sites	Reference
Powder-Tongue	50	9	1	(*51*)
Rio Grande-Elephant Butte	21	19	2	(*52*)
Rio Grande-Mimbres	5	8	1	(*53*)
Upper Pecos	16	43	4	(*53*)
White-Yampa	16	7	6	(*54*)
San Juan	72	7	11	(*52*)
Lower Colorado-Lake Mead	11	24	5	(*53*)
Lower Colorado	52	60	1	(*53*)
Salt	3	39	1	(*53*)
Lower Gila	32	31	3	(*53*)
Central Nevada Desert Basins	14	11	1	(*53*)
Neuse-Pamlico	161	1	1	(*76*)
Lake Ontario and Niagara Peninsula	85	1	3	(*83*)
Lower Gila	3	2	2	(*82*)
Middle Gila	6	2	3	(*82*)
Lower Colorado	2	3	9	(*78*)
Rio Grande-Elephant Butte	10	7	1	(*81*)
Middle Snake	37	22	4	(*79*)
Kentucky-Licking	186	0	10	(*77*)
Middle Gila	10	38	10	(*80*)
Middle Gila	7	46	13	(*80*)
Lower Colorado	2	2	9	(*78*)

Table S3: Classification metrics used to assess the ephemeral mapping model. N is number of sites, TP is the true positive rate, TN is the true negative rate, FP is the false positive rate, and FN is the false negative rate.

Name	**Definition**
Accuracy	$\frac{N_{TP} + N_{TN}}{N_{TP} + N_{TN} + N_{FP} + N_{FN}}$
Sensitivity	$\frac{N_{TP}}{N_{TP} + N_{FN}}$
Specificity	$\frac{N_{TN}}{N_{TN} + N_{FP}}$
True Skill Score (TSS)	Sensitivity + Specificity - 1

Table S4: Field assessments of stream ephemerality performed in New England (Summer 2022). We followed the ephemeral/intermittent/perennial protocol for the State of North Carolina Department of Water Quality (*63*). Scores < 19 are deemed 'ephemeral'.

Name	Latitude	Longitude	Score	Classification
Tucker1	42.95125	-71.07311	5.5	ephemeral
Tucker2	42.94875	-71.07479	15.0	ephemeral
Atkins1	42.41396	-72.46797	16.5	ephemeral
Atkins2	42.42449	-72.48076	8.0	ephemeral
Harkness1	42.36701	-72.47190	12.5	ephemeral

655

References and Notes

1. P. A. Raymond, J. E. Saiers, W. V. Sobczak, Hydrological and biogeochemical controls on watershed dissolved organic matter transport: Pulse-shunt concept. *Ecology* **97**, 5–16 (2016). doi:10.1890/14-1684.1 Medline

2. B. He, S. Kanae, T. Oki, Y. Hirabayashi, Y. Yamashiki, K. Takara, Assessment of global nitrogen pollution in rivers using an integrated biogeochemical modeling framework. *Water Res.* **45**, 2573–2586 (2011). doi:10.1016/j.watres.2011.02.011 Medline

3. L. J. J. Meijer, T. van Emmerik, R. van der Ent, C. Schmidt, L. Lebreton, More than 1000 rivers account for 80% of global riverine plastic emissions into the ocean. *Sci. Adv.* **7**, eaaz5803 (2021). doi:10.1126/sciadv.aaz5803 Medline

4. M. Liu, Q. Zhang, T. Maavara, S. Liu, X. Wang, P. A. Raymond, Rivers as the largest source of mercury to coastal oceans worldwide. *Nat. Geosci.* **14**, 672–677 (2021). doi:10.1038/s41561-021-00793-2

5. T. J. Battin, R. Lauerwald, E. S. Bernhardt, E. Bertuzzo, L. G. Gener, R. O. Hall Jr., E. R. Hotchkiss, T. Maavara, T. M. Pavelsky, L. Ran, P. Raymond, J. A. Rosentreter, P. Regnier, River ecosystem metabolism and carbon biogeochemistry in a changing world. *Nature* **613**, 449–459 (2023). doi:10.1038/s41586-022-05500-8 Medline

6. L. C. Alexander, K. M. Fritz, K. A. Schofield, B. C. Autrey, J. E. DeMeester, H. E. Golden, D. C. Goodrich, W. G. Kepner, H. R. Kiperwas, C. R. Lane, S. D. LeDuc, S. G. Leibowitz, M. G. McManus, A. I. Pollard, C. E. Ridley, M. K. Vanderhoof, P. J. Wigington Jr., Featured Collection Introduction: Connectivity of Streams and Wetlands to Downstream Waters. *J. Am. Water Resour. Assoc.* **54**, 287–297 (2018). doi:10.1111/1752-1688.12630

7. J. Harvey, J. Gomez-Velez, N. Schmadel, D. Scott, E. Boyer, R. Alexander, K. Eng, H. Golden, A. Kettner, C. Konrad, R. Moore, J. Pizzuto, G. Schwarz, C. Soulsby, J. Choi, How Hydrologic Connectivity Regulates Water Quality in River Corridors. *J. Am. Water Resour. Assoc.* **55**, 369–381 (2019). doi:10.1111/1752-1688.12691 Medline

8. M. L. Messager, B. Lehner, C. Cockburn, N. Lamouroux, H. Pella, T. Snelder, K. Tockner, T. Trautmann, C. Watt, T. Datry, Global prevalence of non-perennial rivers and streams. *Nature* **594**, 391–397 (2021). doi:10.1038/s41586-021-03565-5 Medline

9. K. L. Jaeger, R. Sando, R. R. McShane, J. B. Dunham, D. P. Hockman-Wert, K. E. Kaiser, K. Hafen, J. C. Risley, K. W. Blasch, Probability of Streamflow Permanence Model (PROSPER): A spatially continuous model of annual streamflow permanence throughout the Pacific Northwest. *J. Hydrol.* **2**, 100005 (2019). doi:10.1016/j.hydroa.2018.100005

10. N. Durighetto, V. Mariotto, F. Zanetti, K. J. McGuire, G. Mendicino, A. Senatore, G. Botter, Probabilistic description of streamflow and active length regimes in rivers. *Water Resour. Res.* **58**, WR031344 (2022). doi:10.1029/2021WR031344 Medline

11. P. P. Russell, S. M. Gale, B. Muñoz, J. R. Dorney, M. J. Rubino, A spatially explicit model for mapping headwater streams. *J. Am. Water Resour. Assoc.* **51**, 226–239 (2015). doi:10.1111/jawr.12250

12. K. A. Fesenmyer, S. J. Wenger, D. S. Leigh, H. M. Neville, Large portion of USA streams lose protection with new interpretation of Clean Water Act. *Freshw. Sci.* **40**, 252–258 (2021). doi:10.1086/713084

13. C. Cavallo, M. N. Papa, G. Negro, M. Gargiulo, G. Ruello, P. Vezza, Exploiting Sentinel-2 dataset to assess flow intermittency in non-perennial rivers. *Sci. Rep.* **12**, 21756 (2022). doi:10.1038/s41598-022-26034-z Medline

14. S. Greenhill, H. Druckenmiller, S. Wang, D. A. Keiser, M. Girotto, J. K. Moore, N. Yamaguchi, A. Todeschini, J. S. Shapiro, Machine learning predicts which rivers, streams, and wetlands the Clean Water Act regulates. *Science* **383**, 406–412 (2024). doi:10.1126/science.adi3794 Medline

15. J. P. Benstead, D. S. Leigh, An expanded role for river networks. *Nat. Geosci.* **5**, 678–679 (2012). doi:10.1038/ngeo1593

16. E. H. Stanley, S. G. Fisher, N. B. Grimm, Ecosystem expansion and contraction in streams. *Bioscience* **47**, 427–435 (1997). doi:10.2307/1313058

17. R. B. Alexander, E. W. Boyer, R. A. Smith, G. E. Schwarz, R. B. Moore, The role of headwater streams in downstream water quality. *J. Am. Water Resour. Assoc.* **43**, 41–59 (2007). doi:10.1111/j.1752-1688.2007.00005.x Medline

18. K. M. Fritz, K. A. Schofield, L. C. Alexander, M. G. McManus, H. E. Golden, C. R. Lane, W. G. Kepner, S. D. LeDuc, J. E. DeMeester, A. I. Pollard, Physical and chemical connectivity of streams and riparian wetlands to downstream waters: A synthesis. *J. Am. Water Resour. Assoc.* **54**, 323–345 (2018). doi:10.1111/1752-1688.12632 Medline

19. Y. Fan, H. Li, G. Miguez-Macho, Global patterns of groundwater table depth. *Science* **339**, 940–943 (2013). doi:10.1126/science.1229881 Medline

20. Y. Fan, G. Miguez-Macho, E. G. Jobbágy, R. B. Jackson, C. Otero-Casal, Hydrologic regulation of plant rooting depth. *Proc. Natl. Acad. Sci. U.S.A.* **114**, 10572–10577 (2017). doi:10.1073/pnas.1712381114 Medline

21. K. Bieger, H. Rathjens, P. M. Allen, J. G. Arnold, Development and evaluation of bankfull hydraulic geometry relationships for the physiographic regions of the United States. *J. Am. Water Resour. Assoc.* **51**, 842–858 (2015). doi:10.1111/jawr.12282

22. US Geological Survey, National Hydrography Dataset version USGS National Hydrography Dataset High Resolution(NHD-HR) for Hydrologic Unit (HU) 4 (2022); https://www.usgs.gov/national-hydrography/access-national-hydrography-products.

23. C. B. Brinkerhoff, P. A. Raymond, T. Maavara, Y. Ishitsuka, K. S. Aho, C. J. Gleason, Lake morphometry and river network controls on evasion of terrestrially sourced headwater CO2. *Geophys. Res. Lett.* **48**, e2020GL090068 (2021). doi:10.1029/2020GL090068

24. The Clean Water Act. 33 USC. § 1251 (1972).

25. R. Walsh, A. S. Ward, An overview of the evolving jurisdictional scope of the US Clean Water Act for hydrologists. *WIREs. Water* **9**, e1603 (2022). doi:10.1002/wat2.1603

26. D. A. Keiser, J. S. Shapiro, Consequences of the Clean Water Act and the demand for water quality. *Q. J. Econ.* **134**, 349–396 (2019). doi:10.1093/qje/qjy019

27. United States v. Riverside Bayview Homes, Inc. 474 US 121 (1985).

28. Rapanos v. US. 547 US 715 (2006).

29. Department of the Army, Corps of Engineers, Department of Defense, Environmental Protection Agency, Clean Water Rule: Definition of "Waters of the United States." Fed. Reg. **80**, 37054–37127 (2015).

30. Department of the Army, Corps of Engineers, Department of Defense, Environmental Protection Agency, The Navigable Waters Protection Rule: Definition of "Waters of the United States." Fed. Reg. **85**, 22250–22342 (2020).

31. Department of the Army, Corps of Engineers, Department of Defense, Environmental Protection Agency, Revised definition of 'Waters of the United States." Fed. Reg. **88**, 61964–61969 (2023).

32. Sackett v. EPA. 143 US 1322 (2023).

33. D. G. Tarboton, R. L. Bras, I. Rodriguez-Iturbe, The fractal nature of river networks. *Water Resour. Res.* **24**, 1317–1322 (1988). doi:10.1029/WR024i008p01317

34. S. Zanardo, I. Zaliapin, E. Foufoula-Georgiou, Are American rivers Tokunaga self-similar? New results on fluvial network topology and its climatic dependence. *J. Geophys. Res. Earth Surf.* **118**, 166–183 (2013). doi:10.1029/2012JF002392

35. P. S. Dodds, D. H. Rothman, Scaling, universality, and geomorphology. *Annu. Rev. Earth Planet. Sci.* **28**, 571–610 (2000). doi:10.1146/annurev.earth.28.1.571

36. E. Tokunaga, Considerations on the composition of drainage networks. *Geogr. Rep. Tokyo Metrop. Univ.* **13**, 1–27 (1978).

37. T. Gleeson, L. Marklund, L. Smith, A. H. Manning, Classifying the water table at regional to continental scales. *Geophys. Res. Lett.* **38**, n/a (2011). doi:10.1029/2010GL046427

38. L. E. Condon, R. M. Maxwell, Evaluating the relationship between topography and groundwater using outputs from a continental-scale integrated hydrology model. *Water Resour. Res.* **51**, 6602–6621 (2015). doi:10.1002/2014WR016774

39. D. C. Goodrich, W. G. Kepner, L. R. Levick, P. J. Wigington Jr., Southwestern intermittent and ephemeral stream connectivity. *J. Am. Water Resour. Assoc.* **54**, 400–422 (2018). doi:10.1111/1752-1688.12636

40. B. R. Scanlon, C. C. Faunt, L. Longuevergne, R. C. Reedy, W. M. Alley, V. L. McGuire, P. B. McMahon, Groundwater depletion and sustainability of irrigation in the US High Plains and Central Valley. *Proc. Natl. Acad. Sci. U.S.A.* **109**, 9320–9325 (2012). doi:10.1073/pnas.1200311109 Medline

41. S. Jasechko, H. Seybold, D. Perrone, Y. Fan, J. W. Kirchner, Widespread potential loss of streamflow into underlying aquifers across the USA. *Nature* **591**, 391–395 (2021). doi:10.1038/s41586-021-03311-x Medline

42. P. Xie, M. Chen, S. Yang, A. Yatagai, T. Hayasaka, Y. Fukushima, C. Liu, A gauge-based analysis of daily precipitation over East Asia. *J. Hydrometeorol.* **8**, 607–626 (2007). doi:10.1175/JHM583.1

43. J. Brakebill, D. Wolock, S. Terziotti, Digital hydrologic networks supporting applications related to spatially referenced regression modeling1. *J. Am. Water Resour. Assoc.* **47**, 916–932 (2011). doi:10.1111/j.1752-1688.2011.00578.x Medline

44. N. Catalàn, R. del Campo, M. Talluto, C. Mendoza-Lera, G. Grandi, S. Bernal, D. von Schiller, G. Singer, E. Bertuzzo, Pulse, shunt and storage: Hydrological contraction shapes processing and export of particulate organic matter in river networks. *Ecosystems* **26**, 873–892 (2022). doi:10.1007/s10021-022-00802-4

45. S. E. Godsey, J. Hartmann, J. W. Kirchner, Catchment chemostasis revisited: Water quality responds differently to variations in weather and climate. *Hydrol. Processes* **33**, 3056–3069 (2019). doi:10.1002/hyp.13554

46. S. E. Godsey, J. W. Kirchner, D. W. Clow, Concentration-discharge relationships reflect chemostatic characteristics of US catchments. *Hydrol. Processes* **23**, 1844–1864 (2009). doi:10.1002/hyp.7315

47. C. Leigh, A. J. Boulton, J. L. Courtwright, K. Fritz, C. L. May, R. H. Walker, T. Datry, Ecological research and management of intermittent rivers: An historical review and future directions. *Freshw. Biol.* **61**, 1181–1199 (2016). doi:10.1111/fwb.12646

48. Code for: C. B. Brinkerhoff, C. J. Gleason, M. J. Kotchen, D. Kysar, P. A. Raymond, Ephemeral stream water contributions to United States drainage networks, Version 1.2.1, Zenodo (2024); https://doi.org/10.5281/zenodo.10659028.

49. Model results for: C. B. Brinkerhoff, C. J. Gleason, M. J. Kotchen, D. Kysar, P. A. Raymond, Ephemeral stream water contributions to United States drainage networks, Version 2, Zenodo (2024); https://doi.org/10.5281/zenodo.10658663.

50. L. L. DeLong, D. K. Wells, "Estimating average dissolved-solids yield from basins drained by ephemeral and intermittent streams--Green River Basin, Wyoming" (Department of the Interior, US Geological Survey, Report 87-4222, 1988); https://pubs.usgs.gov/wri/1987/4222/report.pdf.

51. J. G. Rankl, "Relations between total-sediment load and peak discharge for rainstorm runoff on five ephemeral streams in Wyoming" (Department of the Interior, US Geological Survey, Report 2002-4150, 2004); https://doi.org/10.3133/wri024150.

52. H. R. Heijl Jr., "Preliminary appraisal of ephemeral-streamflow characteristics as related to drainage area, active-channel width, and soils in northwestern New Mexico" (Department of the Interior, US Geological Survey, Open-File Report 81-64, 1980); https://doi.org/10.3133/ofr8164.

53. R. Schumer, A. Knust, D. P. Boyle, Characteristics of ephemeral hydrographs in the Southwestern United States. *J. Hydrol. Eng.* **19**, 10–17 (2014). doi:10.1061/(ASCE)HE.1943-5584.0000643

54. J. G. Elliott, K. D. Cartier, "Hydraulic geometry and streamflow of channels in the Piceance Basin, Rio Blanco and Garfield Counties" (Department of the Interior, US Geological Survey, Report 85-4118, 1986); https://pubs.usgs.gov/wri/1985/4118/report.pdf.

55. M. A. Zimmer, K. E. Kaiser, J. R. Blaszczak, S. C. Zipper, J. C. Hammond, K. M. Fritz, K. H. Costigan, J. Hosen, S. E. Godsey, G. H. Allen, S. Kampf, R. M. Burrows, C. A.

Krabbenhoft, W. Dodds, R. Hale, J. D. Olden, M. Shanafield, A. G. DelVecchia, A. S. Ward, M. C. Mims, T. Datry, M. T. Bogan, K. S. Boersma, M. H. Busch, C. N. Jones, A. J. Burgin, D. C. Allen, Zero or not? Causes and consequences of zero-flow stream gage readings. *WIREs. Water* **7**, e1436 (2020). doi:10.1002/wat2.1436 Medline

56. E. C. Seybold, A. Bergstrom, C. N. Jones, A. J. Burgin, S. Zipper, S. E. Godsey, W. K. Dodds, M. A. Zimmer, M. Shanafield, T. Datry, R. D. Mazor, M. L. Messager, J. D. Olden, A. Ward, S. Yu, K. E. Kaiser, A. Shogren, R. H. Walker, How low can you go? Widespread challenges in measuring low stream discharge and a path forward. *Limnol. Oceanogr. Lett.* **8**, 804–811 (2023). doi:10.1002/lol2.10356

57. T. C. Winter, J. W. Harvey, O. L. Franke, W. M. Alley, "Ground water and surface water: A single resource" (US Geological Survey, circular 1139, 1998); https://doi.org/10.3133/cir1139.

58. R. G. Niswonger, D. E. Prudic, G. E. Fogg, D. A. Stonestrom, E. M. Buckland, Method for estimating spatially variable seepage loss and hydraulic conductivity in intermittent and ephemeral streams. *Water Resour. Res.* **44**, 2007WR006626 (2008). doi:10.1029/2007WR006626

59. T. A. McMahon, R. J. Nathan, Baseflow and transmission loss: A review. *WIREs. Water* **8**, e1527 (2021). doi:10.1002/wat2.1527

60. Y. Fan, Are catchments leaky? *WIREs. Water* **6**, e1386 (2019). doi:10.1002/wat2.1386

61. B. B. Cael, A. J. Heathcote, D. A. Seekell, The volume and mean depth of Earth's lakes. *Geophys. Res. Lett.* **44**, 209–218 (2017). doi:10.1002/2016GL071378

62. Environmental Protection Agency, "Clean Water Act approved jurisdictional determinations" (EPA, 2023); https://watersgeo.epa.gov/cwa/CWA-JDs/.

63. J. Dorney, P. Russell, "North Carolina Division of Water Quality methodology for identification of intermittent and perennial streams and their origins" in *Wetland and Stream Rapid Assessments*, J. Dorney, R. Savage, R. W. Tiner, P. Adamus, Eds. (Academic, 2018), pp. 273–279.

64. L. E. Condon, S. Kollet, M. F. P. Bierkens, G. E. Fogg, R. M. Maxwell, M. C. Hill, H.-J. H. Fransen, A. Verhoef, A. F. Van Loon, M. Sulis, C. Abesser, Global groundwater modeling and monitoring: Opportunities and challenges. *Water Resour. Res.* **57**, e2020WR029500 (2021). doi:10.1029/2020WR029500

65. I. E. M. de Graaf, E. H. Sutanudjaja, L. P. H. van Beek, M. F. P. Bierkens, A high-resolution global-scale groundwater model. *Hydrol. Earth Syst. Sci.* **19**, 823–837 (2015). doi:10.5194/hess-19-823-2015

66. M. H. Busch, K. H. Costigan, K. M. Fritz, T. Datry, C. A. Krabbenhoft, J. C. Hammond, M. Zimmer, J. D. Olden, R. M. Burrows, W. K. Dodds, K. S. Boersma, M. Shanafield, S. K. Kampf, M. C. Mims, M. T. Bogan, A. S. Ward, M. P. Rocha, S. Godsey, G. H. Allen, J. R. Blaszczak, C. N. Jones, D. C. Allen, What's in a name? Patterns, trends, and suggestions for defining non-perennial rivers and streams. *Water* **12**, 1980 (2020). doi:10.3390/w12071980 Medline

67. J. Wade, C. Kelleher, A. S. Ward, R. L. Schewe, The fluid definition of the "waters of the United States": Non-uniform effects of regulation on US wetland protections. *Hydrol. Processes* **36**, e14747 (2022). doi:10.1002/hyp.14747

68. N. M. Schmadel, J. W. Harvey, G. E. Schwarz, R. B. Alexander, J. D. Gomez-Velez, D. Scott, S. W. Ator, Small ponds in headwater catchments are a dominant influence on regional nutrient and sediment budgets. *Geophys. Res. Lett.* **46**, 9669–9677 (2019). doi:10.1029/2019GL083937

69. S. E. Godsey, J. W. Kirchner, Dynamic, discontinuous stream networks: Hydrologically driven variations in active drainage density, flowing channels and stream order. *Hydrol. Processes* **28**, 5791–5803 (2014). doi:10.1002/hyp.10310

70. O. Allouche, A. Tsoar, R. Kadmon, Assessing the accuracy of species distribution models: Prevalence, kappa and the true skill statistic (TSS). *J. Appl. Ecol.* **43**, 1223–1232 (2006). doi:10.1111/j.1365-2664.2006.01214.x

71. R. E. Horton, Erosional development of streams and their drainage basins; hydrophysical approach to quantitative morphology. *Geol. Soc. Am. Bull.* **56**, 275–370 (1945). doi:10.1130/0016-7606(1945)56[275:EDOSAT]2.0.CO;2

72. J. W. Kirchner, Statistical inevitability of Horton's laws and the apparent randomness of stream channel networks. *Geology* **21**, 591–594 (1993). doi:10.1130/0091-7613(1993)021<0591:SIOHSL>2.3.CO;2

73. L. E. Milton, The geomorphic irrelevance of some drainage net laws. *Aust. Geogr. Stud.* **4**, 89–95 (1966). doi:10.1111/j.1467-8470.1966.tb00055.x

74. K. L. Bowden, J. R. Wallis, Effect of stream-ordering technique on Horton's laws of drainage composition. *Geol. Soc. Am. Bull.* **75**, 767–774 (1964). doi:10.1130/0016-7606(1964)75[767:EOSTOH]2.0.CO;2

75. M. Chen, W. Shi, P. Xie, V. B. S. Silva, V. E. Kousky, R. Wayne Higgins, J. E. Janowiak, Assessing objective techniques for gauge-based analyses of global daily precipitation. *J. Geophys. Res.* **113** (D4), 2007JD009132 (2008). doi:10.1029/2007JD009132

76. M. A. Zimmer, B. L. McGlynn, Bidirectional streamgroundwater flow in response to ephemeral and intermittent streamflow and groundwater seasonality. *Hydrol. Processes* **31**, 3871–3880 (2017). doi:10.1002/hyp.11301

77. K. M. Fritz, G. J. Pond, B. R. Johnson, C. D. Barton, Coarse particulate organic matter dynamics in ephemeral tributaries of a Central Appalachian stream network. *Ecosphere* **10**, e02654 (2019). doi:10.1002/ecs2.2654 Medline

78. S. K. Kampf, J. Faulconer, J. R. Shaw, M. Lefsky, J. W. Wagenbrenner, D. J. Cooper, Rainfall thresholds for flow generation in desert ephemeral streams. *Water Resour. Res.* **54**, 9935–9950 (2018). doi:10.1029/2018WR023714

79. C. W. Slaughter, D. Marks, G. N. Flerchinger, S. S. Van Vactor, M. Burgess, Thirty-five years of research data collection at the Reynolds Creek Experimental Watershed, Idaho, United States. *Water Resour. Res.* **37**, 2819–2823 (2001). doi:10.1029/2001WR000413

80. J. J. Stone, M. H. Nichols, D. C. Goodrich, J. Buono, Long-term runoff database, Walnut Gulch Experimental Watershed, Arizona, United States. *Water Resour. Res.* **44**, 2006WR00573 (2008). doi:10.1029/2006WR005733

81. G. Schoener, Impact of urbanization and stormwater infrastructure on ephemeral channel transmission loss in a semiarid watershed. *J. Hydrol. Reg. Stud.* **41**, 101089 (2022). doi:10.1016/j.ejrh.2022.101089

82. J. C. Stromberg, D. L. Setaro, E. L. Gallo, K. A. Lohse, T. Meixner, Riparian vegetation of ephemeral streams. *J. Arid Environ.* **138**, 27–37 (2017). doi:10.1016/j.jaridenv.2016.12.004

83. S. E. Peirce, J. B. Lindsay, Characterizing ephemeral streams in a southern Ontario watershed using electrical resistance sensors. *Hydrol. Processes* **29**, 103–111 (2015). doi:10.1002/hyp.10136

84. K. M. Fritz, S. Fulton, B. R. Johnson, C. D. Barton, J. D. Jack, D. A. Word, R. A. Burke, Structural and functional characteristics of natural and constructed channels draining a reclaimed mountaintop removal and valley fill coal mine. *J. N. Am. Benthol. Soc.* **29**, 673–689 (2010). doi:10.1899/09-060.1

85. M. A. Zimmer, B. L. McGlynn, Lateral, vertical, and longitudinal source area connectivity drive runoff and carbon export across watershed scales. *Water Resour. Res.* **54**, 1576–1598 (2018). doi:10.1002/2017WR021718

86. E. Moges, B. L. Ruddell, L. Zhang, J. M. Driscoll, L. G. Larsen, Strength and memory of precipitation's control over streamflow across the conterminous United States. *Water Resour. Res.* **58**, e2021WR030186 (2022). doi:10.1029/2021WR030186